Design and evaluation of synthetic bacterial consortia for optimized phenanthrene degradation through the integration of genomics and shotgun proteomics

Marianela Macchi[a], Sabrina Festa[a], Esteban Nieto[a], José M. Irazoqui[b],
Nelson E. Vega-Vela[c,d], Howard Junca[e], María P. Valacco[f], Ariel F. Amadio[b],
Irma S. Morelli[a,g], Bibiana M. Coppotelli[a,*]

[a] Centro de Investigación y Desarrollo en Fermentaciones Industriales, CINDEFI (UNLP, CCT-La Plata, CONICET), La Plata, Argentina
[b] E.E.A. Rafaela, Instituto Nacional de Tecnología Agropecuaria (INTA), CCT Santa Fe, CONICET, Rafaela, Argentina
[c] Pontificia Universidad Javeriana, Bogotá, Colombia
[d] Universidad de Bogotá Jorge Tadeo Lozano, Bogotá, Colombia
[e] Microbiomas Foundation, Div. Ecogenomics & Holobionts, RG Microbial Ecology: Metabolism, Genomics & Evolution, Chía, Colombia
[f] IQUIBICEN, FCEN-UBA, Buenos Aires, Argentina
[g] Comisión de Investigaciones Científicas de la Provincia de Buenos Aires, La Plata, Argentina

ARTICLE INFO

ABSTRACT

Two synthetic bacterial consortia (SC) composed of bacterial strains *Sphingobium* sp. (AM), *Klebsiella aerogenes* (B), *Pseudomonas* sp. (Bc-h and T), *Burkholderia* sp. (Bk) and *Inquilinus limosus* (Inq) isolated from a natural phenanthrene (PHN)-degrading consortium (CON) were developed and evaluated as an alternative approach to PHN biodegradation in bioremediation processes. A metabolic network showing the potential role of strains was reconstructed by *in silico* study of the six genomes and classification of dioxygenase enzymes using RHObase and AromaDeg databases. Network analysis suggested that AM and Bk were responsible for PHN initial attack, while Inq, B, T and Bc-h would degrade PHN metabolites. The predicted roles were further confirmed by physiological, RT-qPCR and metaproteomic assays. SC-1 with AM as the sole PHN degrader was the most efficient. The ecological roles inferred in this study can be applied to optimize the design of bacterial consortia and tackle the biodegradation of complex environmental pollutants.

© 2021 The Authors. Published by Elsevier B.V. This is an open access article under the CC BY-NC-ND license (http://creativecommons.org/licenses/by-nc-nd/4.0/).

1. Introduction

Large amounts of crude oil petroleum components, products and synthetic derivatives are being extracted, burnt and ultimately released into the biosphere every year, a trend that has dramatically increased over the last century due to industrialized crude oil extraction and consumption [1]. Many petroleum compounds like polycyclic aromatic hydrocarbon (PAH) are highly toxic and exhibit low degradation rates. The resulting accumulation of those environmental contaminants exerts negative impacts on human health and ecosystems. In this context, some biologically-mediated technologies are being applied to improve the degradation of pollutants [2,3], considering that entirely controlled degradation bioprocesses are difficult to accomplish

because of the dynamics and intricacy of the microbial communities and the scales required. Thus, consortium-based bioprocesses, in which different specialized microorganisms can efficiently combine various pathways and processes required for the degradation of complex substrates, are being developed and investigated as an alternative biotechnological approach [4]. The design of less complex but equally effective microbial consortia could help improve bioremediation in controlled biodegradation processes [5].

The attributes of resilience, robustness, stress resistance and multi-function make microbial consortia more resistant to environmental perturbations than the isolated strains [6,7]. When studying consortia with biotechnological purposes, it is not only necessary to confirm pollutant degradation efficiency, but also to avoid the accumulation of intermediate metabolites which could be toxic [8,9]. It is also known that measuring cell growth and nutrient uptake of each strain in multi-strain co-culture systems is difficult, presenting a challenge for process establishment [10]. As

---

a consequence, the emerging field of synthetic microbial consortia is playing a critical role in many areas of biodegradation [11]. Synthetic microbial communities enable to construct minimal microbiomes with reduced complexity, allowing researchers to gain mechanistic insights regarding interactions and metabolic exchanges [12,13]. The understanding of the ecological interactions within a consortium will facilitate its successful establishment and function in the target environment, where it will be applied in the bioremediation process.

Genomic, transcriptomic and proteomic techniques applied to the study of consortia are useful to identify key players in degradation, microbial population interactions and behaviour in the face of environmental fluctuations. The *in silico* design of synthetic consortia largely benefits from enhancing the knowledge of microbial metabolism and functional gene annotation, which in turn facilitates the integration of data for better prediction of their behaviour [14,15]. The proteomic assessment of microbial communities is becoming an increasingly utilized approach to describe the underlying mechanisms influencing community development and function [16]. Molecular networks combine different pathways and constitute a framework for interpreting these "omics" data [17]. While these approaches could help to further enhance and optimize natural activities into mixed microbial cultures at ecosystem level [18], their integration will enable original advances in the field of environmental biotechnology [19].

The use of consortia assembled from naturally occurring species is highly interesting because they do not need to be genetically modified and are hence not susceptible to regulatory procedures [20]. In addition, communities built with isolates from the same environment maximize the resemblance to the natural community and preserve the indigenous interactions formed by coadaptation/evolution [21]. This study aims to design synthetic bacterial consortia (SC) highly efficient in polycyclic aromatic hydrocarbon (PAH) degradation by combining the isolated strains of a previously described natural consortium (CON) [22–24] to assess the role of microbial members during biodegradation and obtain a view of bacterial interactions during PAH removal. We examined PHN degradation kinetics and intermediate metabolites and applied omics strategies to study the expression of genes and enzymes involved in PAH degradation pathways in each SC. The results obtained in this work can help us select an efficient consortium to be used as inoculant in soil bioremediation processes and advance in the optimization of bioremediation strategies.

2. Materials and methods

2.1. Bacterial isolates, phylogenetic analyses of the 16S rRNA gene and DNA extraction for genome sequencing

Sphingobium sp. (AM), *Klebsiella aerogenes* (B) and *Pseudomonas* sp. (Bc-h and T) were isolated from a PHN-degrading consortium (CON) obtained from a chronically contaminated soil near La Plata city, Argentina [22]. New efforts were made to obtain more isolates from the other genera previously determined to be present in CON through culture-independent methods, using Mueller Hinton Agar medium supplemented with 6 mg/L colistin antibiotic and EMA medium (yeast extract- mannitol agar). A 100-μl inoculum of a 1/100 CON dilution was plated in duplicate, spread on the surface of the medium with a Drigalsky spatula and incubated for 10 days at around 22 °C. The resulting isolated strains were identified as St5 and St6. The strains were conserved in 40 % glycerol at -80 °C and grown in R3 liquid medium for 24 h before use. DNA extraction and PCR for complete amplification of the 16S rRNA gene were performed according to Festa et al. [22]. Total DNA was extracted

from each isolate for whole-genome sequencing as described by Entcheva et al. [25].

2.2. Whole-genome sequencing, assembly and gene annotation

Genomes of the five isolates were sequenced with Illumina sequencing technology (HiSeq 1500, 2×100-bp paired-end reads) at INDEAR (Rosario, Argentina) and raw data were analysed as described in previous works [23,26]. Draft genome sequences have been deposited at the GenBank nucleotide database under accession nos. **NHOM01** (Bk), **NHON01** (Inq), **MTLB01** (B), **MUIN01** (Bc-h) and **MUHV01** (T). The draft genome sequence of *Sphingobium* sp. AM (**LRUK01**) has been reported in a previous study [23].

2.3. In silico and phylogenetic analyses of aromatic ring-hydroxylating oxygenase (RHO) genes present in the genomes of the isolated strains

The genome sequence of each strain was scanned for the presence of aromatic RHO and other related catabolic genes involved in PAH degradation. The RHObase database was used for aromatic RHO α-subunit gene classification into functional classes (A, B, C and D) as well as for the prediction of substrate specificity [27]. Multiple sequence alignments of the aromatic RHO gene sequences identified in isolate genomes and other homologous genes representative of all known RHO types were performed using CLUSTALX with default settings [28]. The results were then used to construct a tree with the Maximum Likelihood method and the JTT matrix-based model [29] as amino acid replacement model. The robustness of the inferred tree topology was verified by bootstrapping with 1000 replications. Trees were visualized and manipulated using MEGA X Version 10.0.5 [30]. In addition, the AromaDeg database was used to classify genes encoding extradiol dioxygenase proteins (EXDO) [31].

2.4. Metabolic network reconstruction of PHN degradation guided by genomic and phylogenetic data

The enzymes involved in each reaction of the proposed degradation pathways were selected from KEGG database [32] and their amino acid sequences were downloaded from databases with high annotation level, namely RHObase [27] and UniProt [33]. These sequences were compared against the predicted genes in the consortium using BLAST+ [34], with 70 % sequence identity and 70 % query coverage thresholds. For those metabolic steps of a potential pathway where no results were found, we looked for sequences in less specific databases like OrthoDB [35], InterPro [36] and Pfam [37], lowering the identity threshold to 50 %. With all candidates identified, a metabolic network was built using Cytoscape v3.6 [38], where nodes represent the compounds and junctions the enzymes found. Each node can be connected to another by up to six junctions, one for each genome in the consortium. In the case of enzymes with multiple subunits, only the main unit was used in the plot.

2.5. PAH and metabolic intermediate degradation

The use of acenaphthylene, anthracene, benz[a]anthracene, chrysene, dibenz[a,h]anthracene, fluoranthene, fluorene, PHN and pyrene (1 g/L) and 1-hydroxy-2-naphthoic acid (HNA) and salicylic acid (SA) intermediates (100 mg/L) was determined in Liquid Mineral Medium LMM (5 g NaCl, 1 g K_2HPO_4, 1 g $NH_4H_2PO_4$, 1 g $(NH_4)SO_4$, 0.2 g $MgSO_4.7H_2O$ and 3 g KNO_3 per liter of bidistilled water, pH 7) according to Vecchioli et al. [39]. The medium was supplemented with each compound (independently tested as sole carbon and energy source) and assessed in triplicate. All strains

were incubated at 28 °C and 150 rpm for 15 days. A positive growth result was accompanied by the appearance of a brownish colour of oxidized degradation intermediates accumulated in the medium [40]. The quantitative analyses of PHN, HNA and SA degradation (Table S6) and the kinetics of PHN degradation (200 mg/L) (Fig. 4) were performed in triplicate by chemical extraction and measured by HPLC as detailed in our previous works [22,41]. Catechol and 2,3-dihydroxybiphenyl screening methods were performed in LB medium diluted 1/10 with 12.5 μg/mL chloramphenicol, as described in Festa et al. [24].

2.6. Design of synthetic bacterial consortia (SC)

Colonies of every isolate from fresh R3A plates were grown in R3 liquid medium at 28 °C and 150 rpm overnight and then washed with 1 ml of 0.75 % NaCl. The design of SC-1 and SC-4 was carried out by inoculating a volume of cultures of each bacterial strain with the same optical density (OD580 = 0.2) at the beginning of the treatment to ensure similar starting densities. Erlenmeyer flasks (250 ml) containing sterilized LMM supplemented with 200 mg/L PHN were inoculated in triplicate and incubated at 28 °C and 250 rpm. Cultures were monitored at different incubation times for subsequent analyses. A total culture volume of each Erlenmeyer at each sampling time was sacrificed for PAH degradation and RNA isolation analyses, as described below.

2.7. DNA extraction and 16S rDNA sequencing

Total DNA extraction from both designed SC was carried out at different incubation times (0, 4, 7 and 15 days) using the boiling method (Sambrook, Fritsch & Maniatiset, 1989). Paired-end 16S community sequencing was performed with 515 F (GTGY-CAGCMGCCGCGGTAA) - 806R (GGACTACNVGGGTWTCTAAT) primers, targeting the V4 region of the 16S SSU rRNA. DNA concentration was measured with Nanodrop 2000, using 200 ng of each amplicon for library preparation [42]. DNA sequencing was performed on an Illumina Miseq platform (2 × 250 bp) upon established and validated protocols. Bioinformatic analysis was performed as described by Chaves-Moreno et al. [43] using RDP assembler of paired-end reads for quality filtering, trimming and assembly, and DADA2 pipeline, Naive Bayesian Classifier and SILVA 132 as reference databases to define amplicon sequence variants (ASV) and frequencies in all samples. Sequencing data are available at the NCBI Sequence Read Archive (SRA) under accession no. **SUB6478976**.

2.8. RNA isolation and quantitative real-time PCR (RT-qPCR) assays

Cell cultures of the AM strain and SC-1 were grown in LMM supplemented with 200 mg/L PHN and sampled at different incubation times (2, 8, 24, 72 and 96 h) for RNA extraction. Cultures were performed in triplicate. PHN crystals were removed by filtration and cells were then washed, resuspended in RNA later® (Sigma Aldrich) and stored at – 80 °C to prevent RNA degradation. Total RNA extraction was carried out with the RNeasy Protect Bacteria Mini Kit (Qiagen) following the manufacturer's instructions, except that 1 ml guanidine thiocyanate (Trizol® Invitrogen) was added to improve cell lysis. Genomic DNA was removed by incubating one unit of DNasa I (Promega RQ1) per 1 μg of RNA for 45 min at 37 °C. The RNA concentration was calculated by determining the absorbance at 260 nm in NanoDrop 2000 (Thermo-Scientific TM). The quality of RNA was assessed by measuring A260/A280 ratios as well as by electrophoresis in a formaldehyde denaturing agarose gel (1%). The DNA-free RNA was then used as template to synthesize cDNA with M-MLV Reverse

Transcriptase (Invitrogen) and Random Hexamer Primer (Thermo Scientific), following the manufacturers' instructions.

RNA extraction and cDNA synthesis were carried out in independent cultures of each condition run in triplicate. A set of genus-specific primers targeting the 16S rRNA gene of *Sphingobium* sp. genus (AM strain) and genes of the upper and lower PHN degradation pathway were used for RT-qPCR assays (Table S7) [44]. The specificity of primers was verified *in silico* by RAST (Rapid Annotation using Subsystem Technology version 2.0) and Artemis genome browser annotation tools against the AM genome and by PCR with the same programme as detailed below, followed by gel electrophoresis. Melting curves and the efficiency of the selected primer pairs were evaluated by RT-qPCR using qTOWER 2.2 Real-Time PCR Thermal Cycler (Analytik Jena). The reaction mix contained 1 μl of cDNA template, 1 μM of the forward and reverse primers, 0.2 μl of BSA (Sigma) and 2× Power SYBR Green PCR Master Mix (Promega).The cycling parameters of reactions consisted of an initial step of 10 min at 95 °C followed by 45 cycles of denaturation at 95 °C for 15 s, annealing at 72 °C for 75 s and elongation at 72 °C for 5 s. Technical RT-qPCR triplicates of each biological replicate were performed and the relative expression levels were quantified according to the average values. The identity and purity of the amplified product were checked by analysing the melting curve at the end of amplification.

Differences between Cts of each gene of interest were determined in every sample as follows: Ct gene of interest - Ct 16SrRNA gene as reference gene marker. Relative gene expression was quantified with the Delta-Delta Ct method [45] based on the 2-ΔΔCT equation, which assumes that PCR efficiency is close to 1 and PCR efficiency of the target gene is similar to the internal control gene. The expression ratios of the different genes were obtained dividing the normalized power values in the different conditions, using the 2-h condition of each culture as a reference and 16S as reporter gene. Data represent the mean ± STD of biological triplicates and technical triplicates.

2.9. Metaproteome analysis

For protein isolation, SC-1 and SC-4 were grown in LMM supplemented with 200 mg/L of PHN during 72 h in triplicate. Cells from 500 mL of culture were collected by centrifugation at 8000 rpm for 10 min, washed and resuspended in MilliQ water with 5 mM phenylmethylsulfonylfluoride (PMSF) as a protease inhibitor. The cell suspension was disrupted with a Precellys 24-bead beater (Bertin Technologies, location) and solubilized for 1 h in a solubilization solution holding Amberlite. The protein concentration was determined with the Bradford assay using the Bio-Rad Protein Assay Dye Reagent. Protein digestion and mass spectrometry (MS) analysis were performed at the Proteomics Core Facility CEQUIBIEM (University of Buenos Aires-National Research Council), as follows: protein samples were reduced with dithiotreitol (DTT) in 50 mM of ammonium bicarbonate at a final concentration of 10 mM (45 min at 56 °C) and alkylated with iodoacetamide in the same solvent at a final concentration of 30 mM (40 min at room temperature in darkness). Proteins were digested with trypsin (Promega V5111) and peptides were then purified and desalted with ZipTip C18 columns (Millipore).

The digests were analysed by nanoLC-MS/MS in a Thermo Scientific Q Exactive Mass Spectrometer coupled to a nanoHPLC EASY-nLC 1000 (Thermo Scientific). For the LC–MS/MS analysis, approximately 1 μg of peptides was loaded onto the column and eluted for 120 min using an Easy-Spray C18 reverse phase column PepMap RSLC (ES801, 2 μm, 100 A, 50 μm x150 mm), suitable for separating protein complexes with a high degree of resolution. Solvent A was 0.1 % formic acid in water and solvent B was 0.1 % formic acid in acetonitrile (injection volume, 2 μL). Flow rate was

300 nL min^{-1} and solvent B ranged from 7 % (5 min) to 35 % (120 min). The MS equipment has a high collision dissociation cell (HCD) for fragmentation and an Orbitrap analyzer (Thermo Scientific, Q-Exactive). The electrospray ionization voltage applied was 3.5 kV (Thermo Scientific, EASY-SPRAY). XCalibur 3.0.63 (Thermo Scientific) software was used for data acquisition and equipment configuration since it allows peptide identification and chromatographic separation at the same time. Full-scan mass spectra were acquired at a resolution of 70,000 at m/z 400 (mass range, m/z 400–1800) in the Orbitrap analyser. The 12 most intense ions in each cycle were sequentially isolated, fragmented by HCD and measured in the Orbitrap analyser. Peptides with a charge of +1 or unassigned charge state were excluded from MS2 fragmentation.

2.9.1. Data analysis – protein quantitation

The raw data obtained with Q Exactive were processed using Proteome Discoverer software (version 2.1.1.21 Thermo Scientific) and searched against draft genome sequence databases under accession numbers LRUK01 (AM), NHOM01 (Bk), NHON01 (Inq), MTLB01 (B), MUIN01 (Bc-h) and MUHV01 (T), with trypsin specificity and a maximum of one missed cleavage per peptide. The mass spectrometry proteomics data have been deposited to the ProteomeXchange Consortium via the PRIDE [46] partner repository with the dataset identifier PXD022882.

Relative protein abundance in each sample was estimated with the exponentially modified protein abundance index (emPAI) and calculated by Sequest using protein identification data. Protein content in mol% was calculated with the equation emPAI/Σ (emPAI) x 100 [47]. The fold-change values of proteins expressed in both SC were calculated as the emPAI% ratio between CS-1 and CS-4 (emPAI%CS-1/emPAI%CS-4). Protein area data were processed with the Perseus program (Max Planck Institute of Biochemistry, 1.5.5.3 version, available for free) for a deeper statistical analysis. Different scatter plots were done according to the samples compared. For each couple of samples, we plotted the log p value (-Log Student T-test p-value A_B) on the y axis versus the Student T-test Difference A_B in x axis. Proteins that appeared in the volcano plot with a fold change greater than 2 (less than -1 or greater than 1 on the x axis of the graph) and a p value below 0.05 (above 1.3 on the y axis of the graph) were considered as differentially expressed.

2.10. Statistical analysis

The statistical analysis of data was performed with parametric one-way ANOVA, using the SigmaPlot/SigmaStat software programme (SPSS Inc., Chicago, Illinois, USA). Results represent means ± standard deviations.

3. Results

3.1. Isolation, characterization and identification of strains isolated from the natural PHN-degrading consortium (CON)

Taking advantage of their natural interactions, the six CON isolated strains were combined to design the SC and further investigate SC performance and ecological behaviour. Strains *Sphingobium* sp. (AM), *Klebsiella aerogenes* (B) and *Pseudomonas* sp. (Bc-h and T) were characterized by Festa et al. [22]. Based on the knowledge of CON composition already studied by NGS technologies [48], two new strains (St5 and St6) were currently isolated, characterized and identified using different approaches. Supplementary Table S1 summarizes the phenotypic and conventional biochemical characteristics of St5 and St6. Phylogenetic identification by 16S rRNA gene sequence based on a BLASTN search on GenBank showed that the closest matches to strains St5 and St6 were *Inquilinus limosus* and *Burkholderia* sp., respectively, both with 99 % similarity (Table S2). Accordingly, the new isolates were designated Inq (*Inquilinus limosus*) and Bk (*Burkholderia* sp.).

3.2. Genome study of isolated strains and in silico study of genes related to PHN degradation

In order to study the genetic potential of aromatic compound catabolism and identify coding genes related to the PHN degradation pathway, genome analysis of the six isolated strains was carried out. Whole genome shotgun sequencing of each strain produced a draft genome represented by an average of 108 scaffolds and a total estimated median length of 5.56 Mb along with an average of 6018 predicted coding genes. High sequencing coverage (457-fold average coverage) of each genome yielded an N50 contig length of 384,867 bp and a mean G + C content of 62.6 %. The NCBI assembly annotation data are shown in Table S3.
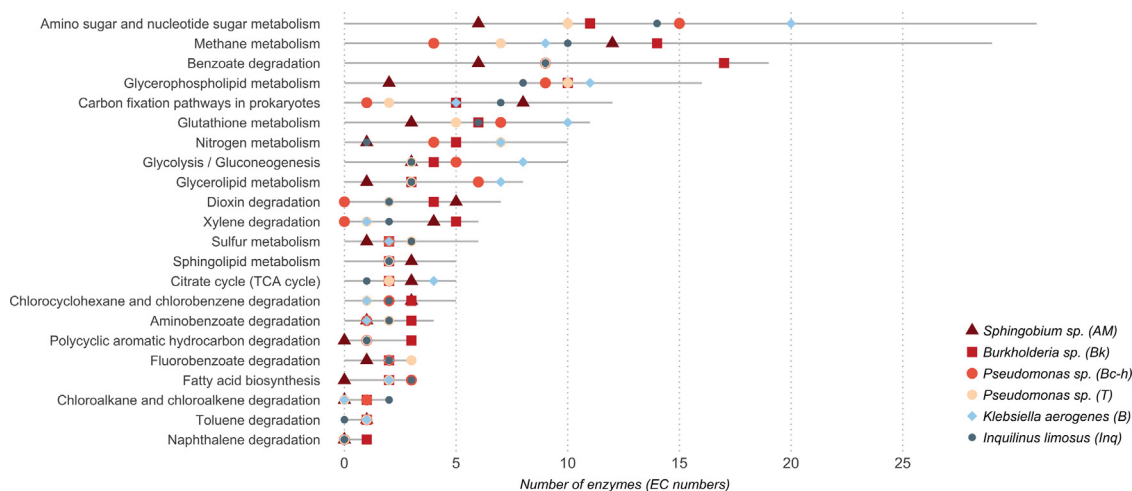
Fig. 1. Number of enzymes per subsystem (KEGG PATHWAY) found in the draft metabolic network reconstructions (obtained from ModelSEED server) of the six taxonomic classes. Gray lines indicate the total enzymes found in each subsystem. (For interpretation of the references to colour in this figure legend, the reader is referred to the web version of this article).

The functional assignment (CDS) of enzymes involved in different steps of the upper and lower PAH degradation pathways of the six isolated strains was based on KEGG. Xenobiotic biodegradation and metabolism reaction predictions were based on RAST and NCBI genome assembly and annotation (Table S4). The analysis of genes responsible for reactions in different metabolic subsystems of the six bacterial genomes is shown in Fig. 1. While Bk possessed a higher number of genes contributing to xenobiotic biodegradation (benzoate, xylene, PAH, cyclohexane) and energy metabolism, the B strain showed a higher number of genes related to general metabolism (carbohydrates, lipids, nucleotides and amino acids). On the other hand, AM possessed a lower number of genes related to general metabolism but a significant number of genes associated with xenobiotic biodegradation (dioxins and xylene).

3.3. Classification of dioxygenase enzymes involved in the upper and lower PAH degradation pathways

To better assess the identification of genes codifying enzymes for PAH initial attack among the isolates, the α-subunit sequences of dioxygenase enzymes were classified into the functional classes of RHObase prediction tool [27]. These enzymes can act in both the upper and lower pathways of PAH degradation. Table S5a shows the RHO classification of enzymes with their putative substrates.

The α subunits of dioxygenase enzyme sequences belonging to the AM and Bk genomes corresponded to the four different RHO functional classes (A, B, C and D), indicating that AM and Bk strains had genomic capability to attack both the upper and lower degradation pathway substrates (aromatic hydrocarbons such as PAH, arylbenzenes and/or alkylbenzenes). In addition, class C RHO were found only in AM and Bk, suggesting that they could catalyse the conversion of salicylate into catechol or gentisate in the lower PHN degradation pathway (Fig. 3). All strains had genes that were classified within the functional classes B and D, having carboxylated aromatic compounds as potential substrates. Additionally, dioxygenase enzymes of Pseudomonas sp. (T and Bc–h) and Inquilinus limosus (Inq) strains were classified as class A (Table S5a). We further studied the phylogenetic relationship between RHO α-subunit amino acid sequences found in the genome of all isolated strains and representative RHO of all known RHO types (Fig. 2). The resulting phylogenetic α-subunit tree confirmed that clustering was broadly associated with substrate specificity. A main branch grouped four dioxygenase enzyme clades (A, B C and D) that were classified within the RHO classification (aromatic ring-hydroxylating enzymes) based on their functional affiliation (Fig. 2).

The AromaDeg database was used to classify genes encoding EXDO in three superfamilies through a phylogenetic approach. These EXDO enzymes cleaved the aromatic ring, had a functional
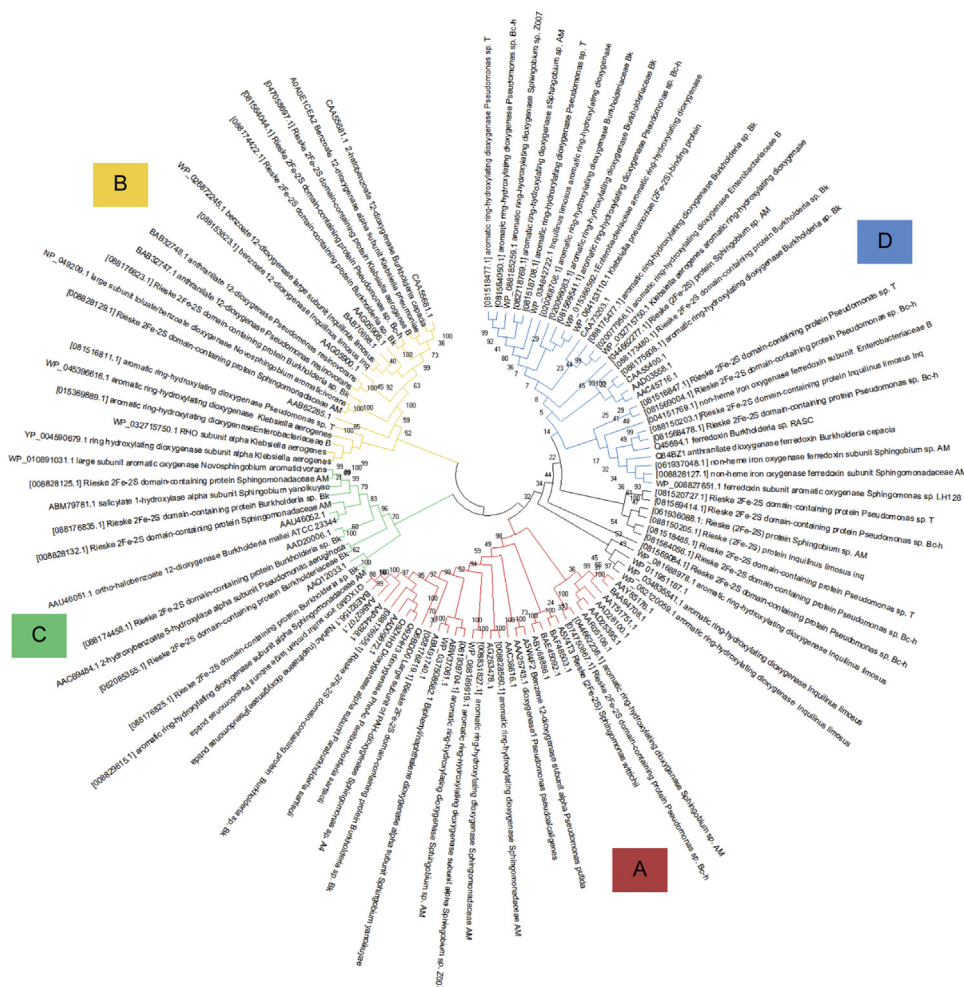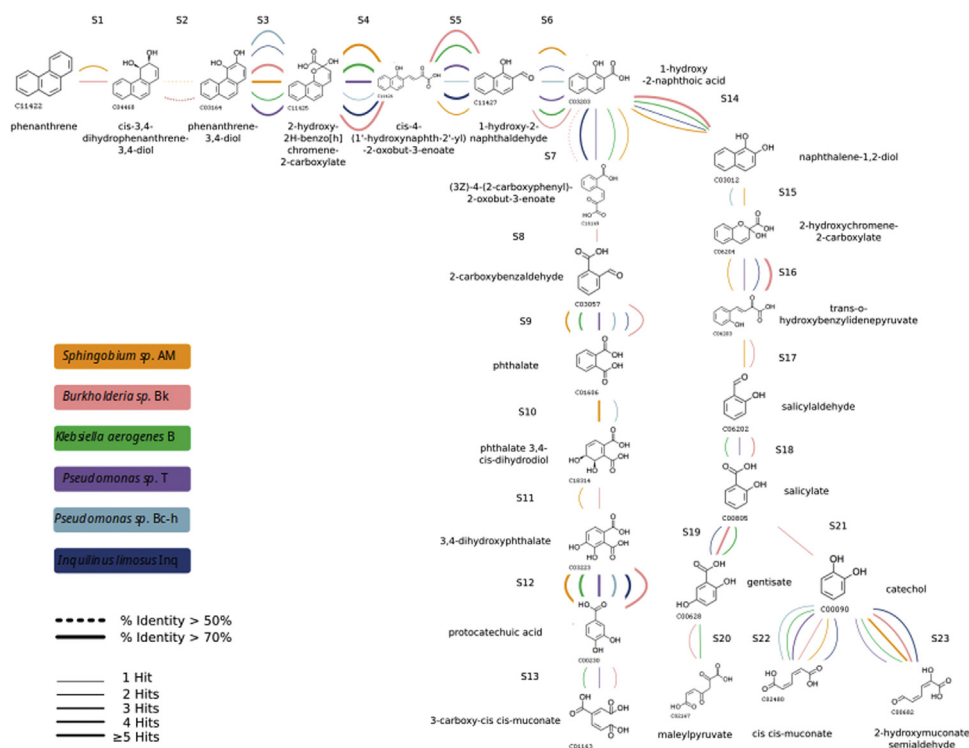

Fig. 2. Maximum Likelihood tree showing phylogenetic relationships between α-subunits of putative RHOs identified in AM, Bk, B, Bch, T and Inq strains (GenBank accession number is shown in brackets) and reference Class A-D Type RHOs. Bootstrapping was performed with 1000 replications.

Fig. 3. Metabolic network graph of enzyme sequences involved in PHN degradation pathway. The width of the line is determined by the number of hits that the corresponding genome contains, while the line type varies according to the threshold of sequence identity used in the search.

convergence regarding the formation of central intermediates and participated in the formation of the hydroxylated derivatives found in the upper and lower pathways of PAH degradation (Table S5b). Both databases demonstrated the presence of genes encoding proteins involved in the upper and lower PAH degradation pathways in the genomes of all strains.

3.4. Metabolic network reconstruction of PHN degradation guided by genomic and phylogenetic data

To understand the role and infer the catabolic capacity of each strain in PHN degradation pathway, the genes involved in different steps of the proposed pathway were analysed using the RAST server and NCBI database. The metabolic network of the PHN degradation pathway constructed using Cytoscape (Fig. 3) shows the integration of genomic and phylogenetic data of the enzymes required to catalyse each step of the degradation pathway (23 steps) for the six isolated strains. The key enzyme 2,3-dihydrox-ybiphenyl 1,2-dioxygenase (EC 1.13.11.39), responsible for PHN initial attack (step 1), was found in AM and Bk genomes. Other dioxygenases such as the alpha and beta subunits of aromatic ring dioxygenase (EC 1.14.12.-), biphenyl 2,3-dioxygenase (EC 1.14.12.18) and naphthalene 1,2-dioxygenase (EC 1.14.12.12), that could act in step 10, were found in all strains. However, only one dioxygenase enzyme (EC 1.13.11.-) that could act in step 7, was found in AM, B, Inq and T strains.

Nearly the complete set of genes encoding the enzymes that would be necessary for PHN degradation by ortho or meta-cleavage pathway was found in strains AM and Bk (Table S4 and Fig. 3), including salicylate-monooxygenase/hydroxylase (EC 1.14.13.1), the main enzyme that could attack HNA (key metabolite in PHN degradation) by meta-cleavage (step 14). Genes for that enzyme were also present in B and Inq strains.

3.5. PAH-degrading capacity of the isolated strains

Considering *in silico* results, we assessed the ability of each strain to degrade a variety of aromatic pollutants in pure cultures, namely PAH, some from the list of priority pollutants of the United States Environmental Protection Agency (EPA) and some metabolic degradation intermediates. Turbidity (reflecting bacterial growth) and yellow/orange colouring (reflecting appearance and accumulation of intermediate metabolites) were considered a positive degradation result. As shown in Table 1, AM and Bk strains were capable of growing and degrading anthracene, fluorene and PHN (1 g/L). Regarding the main intermediates of PHN degradation, AM and Inq degraded HNA (100 mg/L) and only Bk could degrade SA (100 mg/L). Interestingly, Bk, Inq, Bc-h and T strains were able to attack catechol and 2,3-dihydroxybiphenyl, both intermediates of PHN and other PAH degradation pathways.

The quantitative analysis of PHN, HNA and SA degradation carried out after 7 days of incubation showed that AM and Bk were capable of degrading 87.4 ± 4 % [22] and 97 ± 0.8 % of the supplemented PHN, respectively (Table S6). While AM and Inq degraded HNA (43 ± 6 % and 21 ± 4 %, respectively), Bk was the only strain able to use SA as sole carbon source, degrading 92 ± 2 % of the supplemented SA in 7 days. No PHN, HNA or SA degradation was observed in B, Bc-h and T strain cultures.

During PHN degradation, AM and Bk strain cultures accumulated HNA (18.7 ± 0.1 and 11.7 ± 0.6 %, respectively; Fig. 4), but SA was not detected in the culture medium. In particular, HNA remained detectable in Bk cultures until the end of the assay (15 ± 4 mg/L). Even though AM accumulated a higher HNA concentration than Bk, the intermediate was completely degraded at the end of the incubation time. Physiological studies (Table 1) confirmed the predicted roles by *in silico* genomic analysis (Fig. 3), showing a leading activity of AM and Bk in the initial PHN attack.

Table 1

Qualitative analysis of the growth and degradation of different PAH (1 g/L) and intermediate metabolites (100 mg/L) as sole carbon and energy sources in cultures of AM, Bk, Inq, B, Bc-h and T strains, after 15 days of incubation.

PAH and Intermediate metabolites degradation	AM	Bk	Inq	B	Bc-h	T
Acenaphthylene	−	−	−	−	−	−
Anthracene	+	+	−	−	−	−
Benz[a]anthracene	−	−	−	−	−	−
Chrysene	−	−	−	−	−	−
Dibenz[a,h]anthracene	−	−	−	−	−	−
Fluoranthene	−	−	−	−	−	−
Fluorene	+	+	−	−	−	−
Phenanthrene	+	+	−	−	−	−
Pyrene	−	−	−	−	−	−
1-hydroxy-2-naphthoic acid	+	−	+	−	−	−
Salicylic acid	−	+	−	−	−	−
Catechol	−	−	+	−	+	+
2,3-dihydroxybiphenyl	−	+	+	−	+	+

+: positive degradation, −: degradation not detected.

Although in a previous section, dioxygenase enzymes of T, Bc-h and Inq strains were classified as class A (Table 5Sa), degradation studies (Table 1) demonstrated that these strains did not degrade any of the studied PAH. Enzymes of the upper PHN degradation pathway (encoded in AM and Bk strain genomes) would be complemented with enzymes encoded in T, Inq and Bc-h strain genomes that participate in subsequent steps and mainly in the lower pathway, attacking compounds such as HNA, catechol or 2,3-dihydroxybiphenyl (Table 1).

3.6. Design, characterization and comparative PHN biodegradation and HNA production of SC

Considering previously obtained results, two SC containing all the isolated strains were designed and their degradation performance studied with the aim of evaluating individual roles and optimizing the design of efficient consortia in PHN degradation. The two designed consortia were SC-1, composed of five strains (AM, B, T, Bc-h and Inq) and SC-4, composed of all six strains (AM, B, Bc-h, T, Inq and Bk).

The qualitative analysis of PAH degradation revealed the production of coloured intermediate metabolites in SC-1 and SC-4 after 15 days of incubation with 100 mg/L anthracene, fluorene and PHN. However, none of the SC were able to degrade acenaphthylene, chrysene and pyrene under the studied conditions (data not shown).

Phenanthrene degradation kinetics in LMM supplemented with 200 mg/L PHN and HNA production were studied in SC-1 and SC-4 and compared with CON and axenic cultures of AM and Bk strains
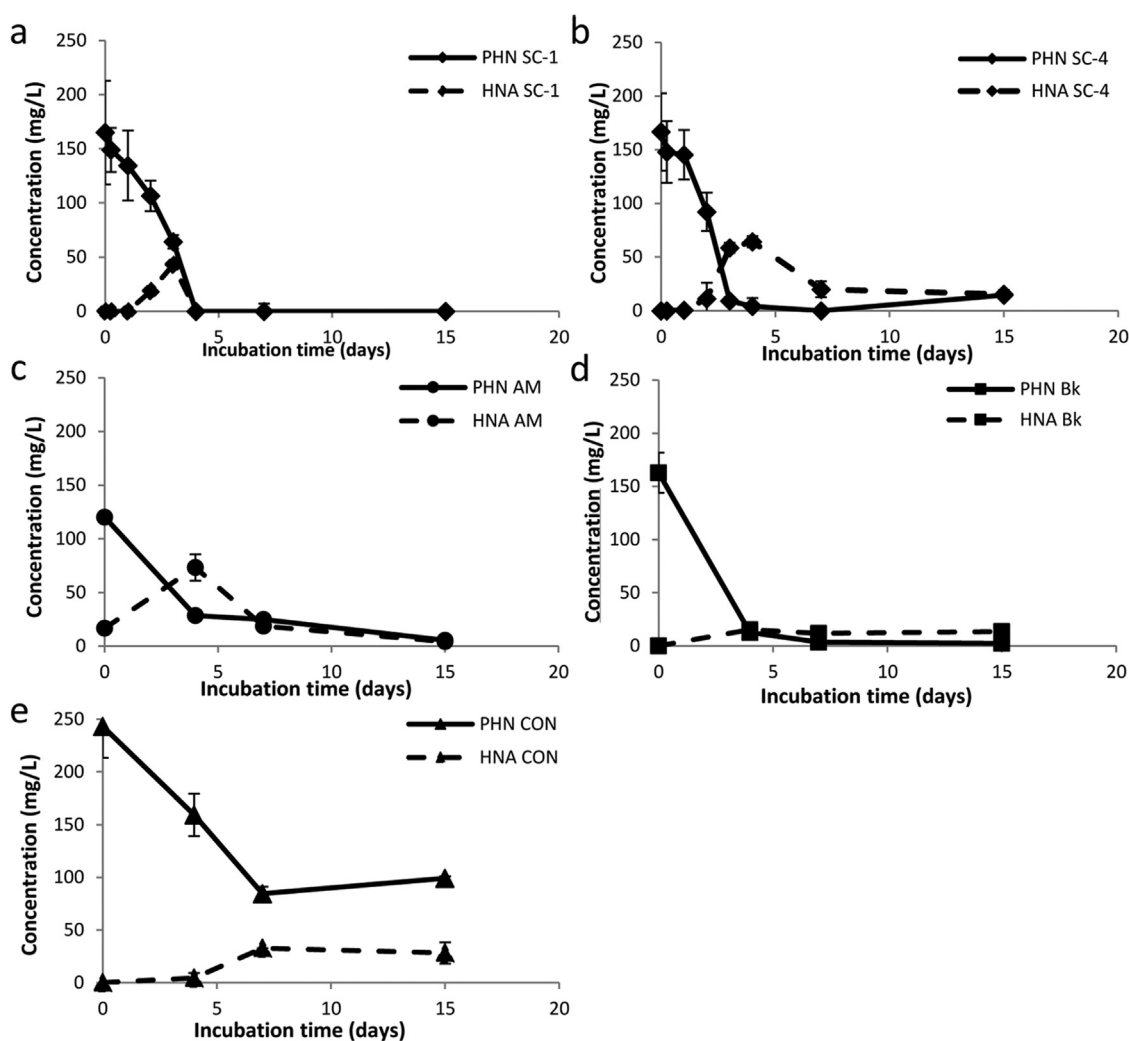
Fig. 4. Phenanthrene (PHN) and 1-hydroxy-2-naphthoic acid (HNA) concentration in **a**) SC-1, **b**) SC-4, **c**) AM strain, **d**) Bk strain and **e**) CON consortium grown in LMM with PHN as sole carbon and energy source (200 mg/L) during 15 days of incubation. Results are means of independent experiments performed in triplicate. Bars represent standard deviations.

at different incubation periods (Fig. 4). Both SC-1 and SC-4 presented a significantly higher degradation efficiency (P < 0.05; Fig. 4**a** and **b**) than AM and Bk (Fig. 4**c** and **d**) and CON (Fig. 4**e**) after 4 days of incubation. While SC-1 and SC-4 were able to degrade more than 99 % of the supplemented PHN within 7 days of incubation, CON degraded only 65 %. Also, AM and Bk reached 88 % and 97 % degradation, respectively, after 7 days (Fig. 4**c** and **d**) and were more effective in degrading PHN than CON (65 %) (Fig. 4**e**). Although CON exhibited good biodegradation performance during the first 7 days of incubation, thereafter the PHN concentration remained constant.

The production and accumulation of HNA were detected in all systems around day 4 (Fig. 4, dotted lines). While HNA production was higher in SC-4 (58 ± 4 mg/L) than SC-1 (42 ± 3 mg/L) by day 3, HNA accumulation in SC-1 (with AM as the sole degrader) was observed until day 3 and was then eliminated, reaching not detectable concentrations at day 4. In the case of SC-4, which contained AM and Bk PHN-degrading strains, it showed a different pattern of HNA production and elimination. The intermediate increased until day 4, decreased towards day 7 to values around 20 ± 7 mg/L and remained constant until the end of the assay. The final HNA concentration in SC-4 cultures (Fig. 4**b**) was similar to the one obtained in Bk strain cultures (15 ± 4 mg/L) under the same conditions (Fig. 4**d**), and significantly different from that in SC-1 cultures (Fig. 4**a**). Bk and CON exhibited a similar HNA accumulation behaviour throughout the assay, although CON reached a higher residual concentration (28 ± 10 mg/L) that remained at the end of the incubation period (Fig. 4**e**).

3.7. Bacterial population dynamics/evolution

The 16S rRNA gene sequencing was carried out in SC in order to study population dynamics during PHN degradation, tracking the inoculated components at each consortium. Key target orders were *Sphingomonadales* for *Sphingobium* sp. AM, *Enterobacteriales* for *Klebsiella aerogenes* B, *Burkholderiales* for *Burkholderia* sp. (Bk), *Rhodospirillales* for *Inquilinus limosus* Inq and *Pseudomonadales*, comprising strains *Pseudomonas* sp. Bc-h and T. As expected, all exhibited high relative frequencies and showed a unique and predominant amplified sequence variant (ASV) classified with the target affiliation, with the notable exception of the ASV in *Rhodospirillales* (*Inquilinus* genus). No significant changes in relative abundances were observed in SC-1 during the whole assay, being *Pseudomonadales* (ASV 5) (46 %) predominant until day 15 of incubation (Fig. 5**a**). In SC-4, *Sphingomonadales* (ASV 3) (31 %) and *Pseudomonadales* (ASV 5) (30 %) were the most abundant orders at the beginning of the assay, with a significant increase of *Burkholderiales* (ASV 81) (36 %) at the end of incubation (Fig. 5**b**).

3.8. Metaproteomic analysis

Metaproteome composition analysis is an excellent tool to properly assess the contribution of different protein functions and their dynamic regulations in a consortium. In order to get a detailed view into the molecular mechanisms modulating PHN degradation, metaproteomes of the studied SC were compared. The analysis specifically focused on proteins related to PAH degradation, stress response when facing the presence and metabolism of those contaminants, and membrane transport proteins potentially involved in the flux of those hydrocarbons. Around 1579 and 1622 proteins were identified in CS-1 and CS-4, respectively, whose total contribution to the studied subsystems (PAH degradation, stress response and membrane transport) did not differ significantly between both consortia (Suppl. Fig. S2). The relative abundance of each identified protein in CS-1 and CS-4 regarding the three subsystems (emPAI%) is shown in Tables S9 and
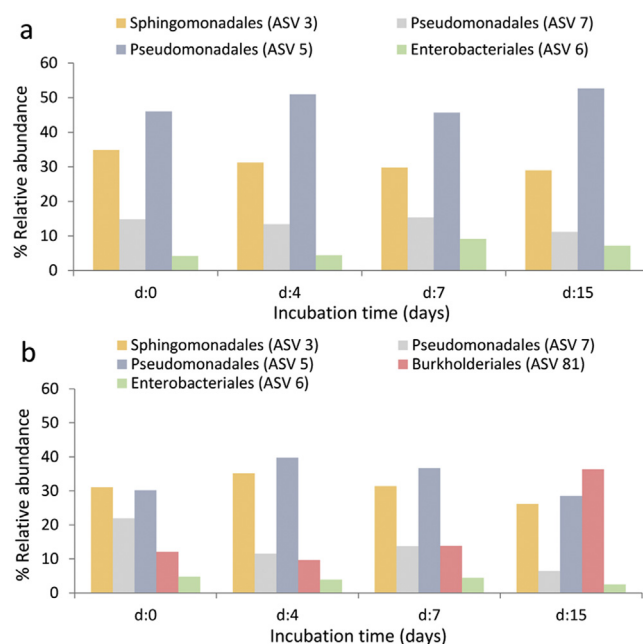
Fig. 5. Dynamics of bacterial population relative abundance in SC-1 (**a**) and SC-4 (**b**) during phenanthrene degradation at order level. Results are means of duplicate independent experiments. Bars represent standard deviations. [*] Significant differences (P < 0.05).

S10 and Fig. 6**a**, **c** and **d**. The contribution percentage of the six strains to each subsystem in CS-1 and CS-4 is shown in Fig. 6**a**. As can be seen, proteins belonging to the five bacterial genera were expressed in both consortia at 72 h during PHN degradation. In addition, Bk presence in SC-4 influenced the protein expression of the other five strains. Particularly, an increase in AM proteins related to PAH degradation and stress resistance was observed when Bk was present (Fig. 6**a**). Dioxygenase enzymes of AM were detected in both consortia in all the steps of the PHN pathway (Fig. 6**c** and **d** and Tables S9 and S10). Simultaneously, homogentisate 1,2-dioxygenase (EC 1.13.11.5) from T and Bc-h, that could act in step 15 (Table S4), was also detected in CS-1 and CS-4 (Fig. 6**b**–**d** and Tables S9 and S10).

A linear model for the statistical evaluation of the results obtained from mass spectra of the total proteins of both SC was created to reveal the distribution of significantly and differentially expressed proteins involved in PAH degradation and other cellular systems (Fig. 6**b**, Volcano plot). The plot was based on the significant difference between acquired proteins (p-value threshold of 0.05 (−log[p value] = 1.301) and a log2 ratio higher than +1, or lower than −1) in SC-1 and SC-4 (Fig. 6**b**). In addition, fold change was calculated to compare the relative abundance of proteins in both consortia. Differentially expressed proteins are described in Fig. 6**b** and **c** and Table S10, and proteins detected in only one of the two consortia are illustrated in Fig. 6**d** (Table S9).

In SC-1, there was a significant up-regulation of proteins involved in PAH degradation, particularly dehydrogenase proteins of AM, B, T and Bc-h strains that could act in steps 2, 6, 9, 11 and 18 (Table S4). Moreover, two proteins of the T strain, homogentisate 1,2-dioxygenase (EC 1.13.11.5) and 4-hydroxyphenylpyruvate dioxygenase (EC 1.13.11.27), were found to be significantly over-expressed (Fig. 6**b** and **c** and Table S10). These two proteins also belonged to an alternative PHN degradation pathway different from the one used from KEGG as reference (Fig. 3). Regarding overexpressed proteins involved in oxidative stress resistance, the higher contribution to SC-1 was from those produced by the B strain, with glyceraldehyde-3-phosphate dehydrogenase (EC
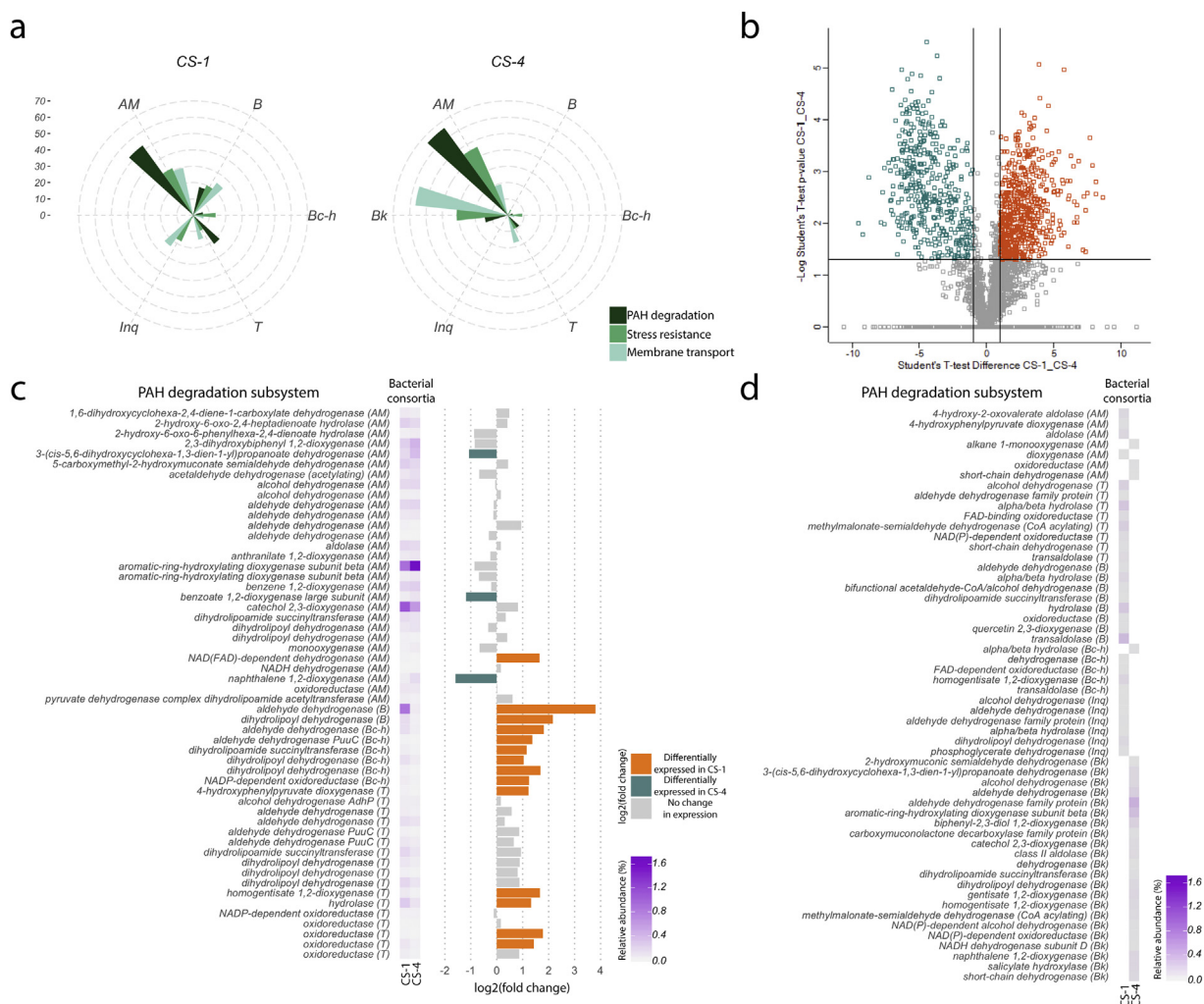
Fig. 6. a Polar circle graphics showing contribution percentage (emPAI) of the six strains to PAH degradation, stress resistance and membrane transport subsystem in CS-1 and CS-4. **b** Volcano plot of protein abundance differences as a function of statistical significance with fold-changes greater than 2 (less than −1 in SC-4 or greater than 1 in SC-1 on the x axis of the graph) and with t-test p-values lower than 0.05 (of values greater than 1.3 on the y axis of the graph). The colour code indicates significantly expressed proteins in SC-1 (orange) and SC-4 (green). Proteins with no statistically significant difference in abundances between the two lineages are shown in gray. **c** Heatmap of proteins present in both consortia involved in PAH degradation (emPAI%) and fold-change between CS-1 and CS-4. The fold-change values of the CS-1/CS-4 ratio (emPAI%CS-1/emPAI%CS-4) were considered significant with fold-changes greater than 2 (overexpressed in CS-1) and lesser than 0.5 (overexpressed in CS-4). **d** Heatmap of proteins detected in a unique consortium (emPAI%) (For interpretation of the references to colour in this figure legend, the reader is referred to the web version of this article).

1.2.1.12), superoxide dismutase (EC 1.15.1.1) and catalase/peroxidase (EC 1.11.1.6) (Fig. 6**b** and Table S10). The other four strains had a minor contribution, with superoxide dismutase (EC 1.15.1.1), glutathione S-transferase (EC 2.5.1.18) and glutathione reductase (EC 1.6.4.2) (Tables S9 and S10). In relation to membrane transporters, overexpressed proteins belonged to the five constituent strains of SC-1 (Fig. 6**b** and Table S10). Transporters like TonB-dependent receptor were mainly contributed by the AM strain and ABC transporters (EC 7.4.2.-) were mainly contributed by the other strains (Fig. 6**b** and Table S10).

On the other hand, expressed proteins of *Burkholderia* sp. (Bk) dominated the three metabolic systems analysed in SC-4 (Fig. 6**b** and Table S10). When considering proteins related to PAH degradation, the detected Bk strain proteins were aromatic-ring-hydroxylating dioxygenase beta subunit (EC 1.14.12.-) (steps 1 and 10), biphenyl-2,3-diol 1,2-dioxygenase (EC 1.13.11.39) (step 10), naphthalene 1,2-dioxygenase (EC 1.14.12.12) (step 10), classified as A in RHObase, and salicylate hydroxylase (EC 1.14.13.1) (steps 14 and 19), classified as B in RHObase, homogentisate 1,2-dioxygenase (EC 1.13.11.5) (step 15) and catechol 2,3-dioxygenase (EC 1.13.11.2) (step 23) (Fig. 6**d**). Also, dioxygenase proteins of AM were

significantly overexpressed in SC-4, like naphthalene 1,2-dioxygenase (EC 1.14.12.12) (step 10), classified as A in RHObase, and benzoate 1,2-dioxygenase large subunit (EC 1.14.12.10) (step 10), classified as B (Fig. 6**b** and **c**). Among dehydrogenase enzymes, several (8) aldehyde dehydrogenases (EC 1.2.1.3) (step 9), 2-hydroxymuconic semialdehyde dehydrogenases (EC 1.2.1.60) (step 18), alcohol dehydrogenases (EC 1.1.1.1) and dihydrolipoyl dehydrogenases (EC 1.8.1.4) (that could act in alternative PHN degradation pathways) belonging to Bk were detected in CS-4 (Fig. 6**b**, **d** and Table S10). The increased relative abundance of proteins related to stress resistance in SC-4, like glutathione S-transferase (EC 2.5.1.18), catalase (EC1.11.1.6) and superoxide dismutase (EC 1.15.1.1), belonged entirely to the Bk strain. Additionally, most of the proteins related to membrane transport (like ABC transporters) belonged to Bk and T strains (Fig. 6**b** and Tables S9 and S10).

3.9. RT-qPCR analyses

The relative expression levels of the AM strain specific genes (upper and lower PAH degradation pathway; Table S7) were
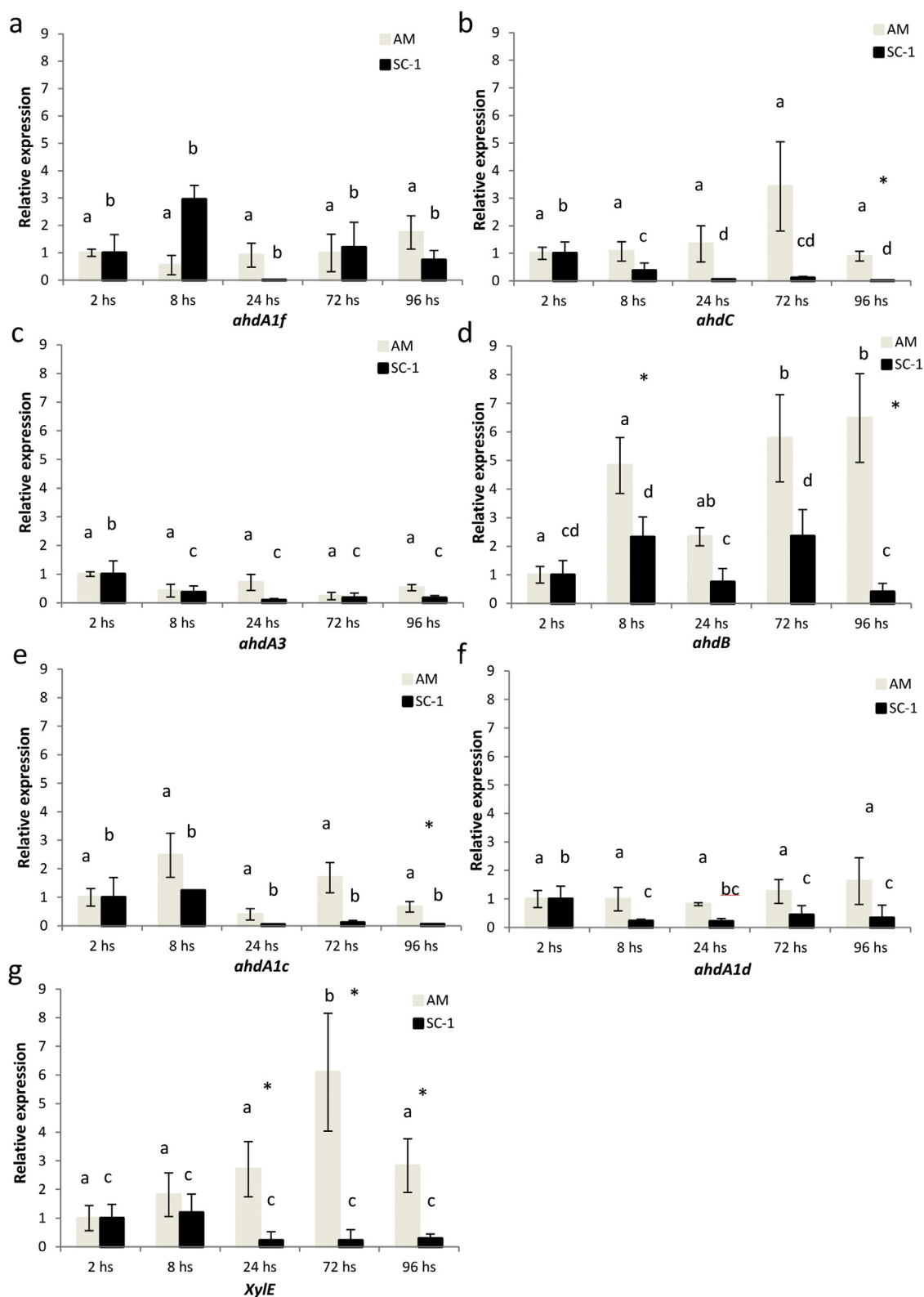
Fig. 7. Relative expression values of key genes regulated during phenanthrene degradation in AM and SC-1 cultures (**a**: *ahdA1f*, **b**: *ahdC*, **c**: *ahdA3*, **d**: *ahdB*, **e**: *ahdA1c*, **f**: *ahdA1d* and **g**: *XylE*). The values are expressed as 'fold change' and represent the ± STD averages of biological triplicates and technical triplicates and indicate the change in mRNA levels of the studied genes compared with the control conditions (value of 1). Significant differences in gene expression between conditions (different times) of the same culture (AM or SC-1) are shown with different letters (a, b, c and d) and significant differences between cultures (AM and SC-1) for each time are shown with an asterisk (*). The Student's test was used, setting significance at ± 0.05 (two-way ANOVA, Tukey test). Error bars correspond to standard deviations.

compared in axenic AM and SC-1 cultures during PHN degradation (2, 8, 24, 72 and 96 h). We progressed in the analysis of SC-1 since it was the most efficient in degrading PHN and because intermediate HNA was not detected after day 4 of incubation.

Large subunit naph/bph dioxygenase (ahdA1f) and 2,3-dihydroxybiphenyl 1,2-dioxygenase (ahdC) were the primers used in RT-qPCR analysis of genes encoding enzymes for the first step of the upper PHN degradation pathway; large toluate/benzoate dioxygenase subunit (ahdA1c and ahdA1d) and catechol 2,3-dioxygenase (xylE) were used for genes encoding enzymes for the lower pathway. We also used primers for genes encoding enzymes that could participate in both upper and lower PHN degradation pathway, such as dihydrodiol dehydrogenase (ahdB), ferredoxine and ring-hydroxylating dioxygenases (ahdA3).

Fig. 7 shows the mRNA fold change of ahdA1f, ahdC, ahdA3, ahdB, ahdA1c, ahdA1c, ahdA1d and XylE genes in samples from axenic cultures of the AM strain compared with cultures of SC-1 samples at different times during PHN degradation in relation to the internal control (16 s rRNA gene specific for Sphingomonas genus) using the Delta-Delta Ct method. The gene expression of AM (gray bars) and SC-1 (black bars) is shown in relation to the expression at 2 h of incubation (value of one). All genes studied in AM were found to be expressed after 2 h of incubation (control condition), while most of the analysed genes did not show significant changes until the end of the assay. The expression of ahdC, ahdB, ahdA1c and XylE genes when PHN and HNA were consumed (at 96 h of incubation) was significantly down-regulated in SC-1 as compared with AM (Fig. 7b, d, e and g). The expression of adhA1c (96 h) and XylE (72 and 96 h) genes (both acting in the lower pathway of degradation) was significantly down-regulated in SC-1 compared with AM (P < 0.05; Fig. 7e and g), suggesting a weak participation of AM in the lower degradation pathway when being part of SC-1. This could be explained by the presence of other strains (T, Bc-h and Inq) able to participate in the low degradation pathway, as was described in Table 1.

4. Discussion

When designing synthetic consortia, the lack of adaptation of allochthonous populations can often endanger their survival [49]. The selection of populations pre-adapted to function together is essential to minimize the ecological interactions that could interfere with their behaviour. The study of interactions between members as well as of their adaptability and potential roles in the community is fundamental to open the door to understanding bacterial consortia functioning [50] and could help to optimize their design for remediation purposes.

The strategies applied in this work to isolate all the members of the natural consortium CON obtained by Festa et al. [22] yielded two new isolates, Inquilinus limosus (Inq) and Burkholderia sp. (Bk) (Table S2). The Bk strain showed an efficient PHN degradation and other three-ring PAHs in pure cultures (Table 1), which is in line with the widely reported ability of the Burkholderiales order to degrade aromatic compounds [51,52]. On the other hand, despite the Inq strain did not degrade any of the studied PAHs, it showed degradation of intermediates such as HNA, catechol and 2,3-dihydroxybiphenyl (Table 1), indicating its possible participation in the lower degradation pathway (Fig. 3). To date, no PAH-degrading bacteria belonging to the Inquilinus order have been reported.

A number of gene families encoding enzymes act on critical steps of the aerobic and anaerobic degradation of polyaromatic hydrocarbons [53]. It is well established that there are two critical steps in the aerobic biodegradation of PAH, one involving the α subunit of the Rieske non-heme iron ring-hydroxylating dioxygenases [54,55] and another involving EXDO [56].

Several genes encoding enzymes for the upper and lower PHN degradation pathway were found in the genomes of the six different populations composing the consortia through the in silico analysis of encoding genes related to PAH degradation pathways (Table S5a and b, Fig. 2 and Table S4). The resulting tree, based on the phylogenetic relationship of dioxygenase enzyme sequences, showed that all RHO dioxygenases characterized in the consortium were grouped according to their substrate specificity (Fig. 2). The RHObase classification (Table S5a) indicated that AM and Bk were essential for the initial PHN attack since key (class A) dioxygenase enzymes that can participate in the first step of aromatic ring cleavage (Table S5a) were found in their genomes (they possessed the highest gene copy number of initial dioxygenase enzymes) (Table S4). This is concordant with the physiological analysis where AM and Bk demonstrated to be the only strains able to degrade PHN and other PAH in pure cultures (Table 1). These strains were also the only ones containing genes codifying for class C enzymes (Table S5a), which were responsible for catalysing the conversion of salicylate into catechol or gentisate in the lower PHN degradation pathway (steps 19 and 21; Fig. 3). This result was confirmed only for Bk in the physiological analysis (Table 1). The discrepancy with Sphingobium sp. AM can be based on an operon regulation, considering that Khara et al. [44] suggested that the expression of catabolic enzymes of aromatic compounds requires multiple inducers. Although catechol degradation was not observed in AM and Bk strains (Table 1), EXDO were classified as EXDO I (Table S5b), indicating that these strains would degrade salicylic acid via gentisate (step 19; Fig. 3). In the case of dioxygenase enzymes of strains T and Bc-h, they were classified as class A (Table S5a). Even though they did not degrade any of the PAH studied, they were able to grow in PHN cultures [22] and degrade intermediate metabolites of PHN and other PAH degradation pathways (Table 1). Cho et al. [57] demonstrated that Pseudomonas strains may require metabolic induction for PHN degradation, since the addition of three different intermediate metabolites (1-hydroxy-2-naphthoate, salicylate, and catechol) as exogenous inducers enhanced PHN degradation. Another factor influencing degradation could be the deficiencies in the transport mechanism, where the substrate cannot enter the cell [58]. The classification of dioxygenases and EXDOs from T, Bc-h, B and Inq strains indicated substituted bicyclic and monocyclic compound specificity (classes B and D, EXDO II and III) (Table S5a and b). Physiological studies demonstrated that Inq, Bc-h and T were able to attack catechol and 2,3-dihydroxybiphenyl (Table 1), suggesting that these strains would participate in the lower PAH degradation pathway.

The HNA degrading potential of all strains at genomic and physiological level was studied due to HNA accumulation during PHN degradation and the well-known interference of this metabolite in the bioremediation process [59,60]. Salicylate hydroxylase, the enzyme responsible for HNA attack, has been little studied [61,62], but its great abundance and diversity in a metagenomic library constructed from a soil contaminated with fuel indicates its importance for aromatic degradation [63]. In our study, the homologous gene sequences of salicylate hydroxylase that could attack HNA by meta-cleavage (step 14; Fig. 3) were found in AM, Bk, B and Inq genomes (Fig. 3 and Table S4). However, only AM and Inq showed degradation of the intermediate in pure cultures (Table 1). Comparison of PHN degradation kinetics in AM and Bk (Fig. 4c and d) showed that both strains quickly degraded more than 95 % of the hydrocarbon after 15 days of incubation. During PHN degradation, Bk accumulated less HNA than AM (Fig. 4c and d), and although AM managed to eliminate more than 98 % of the intermediate at the end of the assay (Fig. 4c), HNA remained in Bk cultures until the end of incubation.

Physiological (Table 1) and genomic (Fig. 3) analysis results suggest that the induction of the enzymes necessary for HNA degradation in Bk, T and Bc-h strains could be attributed to PHN or to the fact that the strains were not able to degrade this intermediate because it cannot enter the cell as an exogenous substrate. Puntus et al. [64] reported that *Burkholderia* sp. was not able to grow from exogenous HNA and accumulated this intermediate when grown in PHN, indicating the existence of unknown regulatory mechanisms. On the other hand, some studies reported that *Pseudomonas* grew in HNA [65,66].The analysis of an active set of reactions mediated by the different strains and the metabolic connections specific for PHN degradation (Fig. 3) indicated that the initial PHN attack could be performed by AM and Bk populations, while Inq, T and Bc-h would intervene later, as confirmed by physiological and proteomic analyses (Table 1 and Fig. 6). Functional redundancy between the consortium populations (Fig. 3) was observed at the lower PHN pathway. Functional redundancy is based on the observation that some species perform similar functions in communities and ecosystems, and can be therefore substituted with little impact on ecosystem processes, with the need to ensure resilience to environmental disturbance [67,68].

Synthetic bacterial consortia SC-1 and SC-4 accelerated PHN degradation, reaching an elimination greater than 99 % on day 7 of incubation (Fig. 4**a** and **b**). Such elimination was significantly higher than the one obtained in CON cultures (65 %) (Fig. 4**e**) and individual cultures of AM (88 %) and Bk (97 %) (Fig. 4**c** and **d**), demonstrating the existence of syntrophic relationships among members. This behaviour has been previously observed in pairwise combinations of CON isolated strains, resulting in a good performance in PHN degradation [22]. Also, Vaidya et al. [69] reported a consortium comprising three bacterial species (*Pseudomonas* sp., *Burkholderia* sp. and *Rhodococcus* sp.) that could effectively degrade 99 % of the supplemented pyrene. Other authors demonstrated that the synergistic and cooperative interactions present in a consortium obtained from mangrove sediments improved pyrene biodegradation [70]. The data suggest that microbes involved in syntrophic interactions have developed molecular mechanisms to establish specific partnerships and interspecies communication, resulting in efficient metabolic cooperation.

The kinetics of HNA in SC-1 (Fig. 4**a**) and SC-4 (Fig. 4**b**) during the first 4 days of incubation showed an accumulation pattern that resembled that of the AM strain, with a higher initial production rate and subsequent degradation. Taking into account the composition of SC-1, where AM was the only strain with genomic and functional capacity to generate the initial PHN attack (Table 1 and Fig. 3), we inferred that AM would participate in the first steps of the pathway. This was corroborated in the metaproteomic analyses through the significant protein expression of *Sphingobium* sp. AM in SC-1 in all steps of the pathway (Fig. 6**a** and Table S10). On the other hand, the lower HNA concentration reached by SC-1 as compared with the AM strain would indicate a synergistic effect with the other strains (Bc-h, B, T and Inq), which would participate in the degradation of PHN metabolites, as shown by the physiological results (Table 1). The participation of *Pseudomonas* sp. T and Bc-h was also demonstrated by the metaproteomic results, since a significant enzyme expression for the lower pathway was observed in SC-1 (Table S10). Concordantly, RT-qPCR assays showed that the expression of *XylE* and *adhA1c* genes (encoding enzymes for the lower pathway of PHN degradation) was significantly down-regulated in SC-1 as compared with AM ($P < 0.05$; Fig. 7**e**–**g**), suggesting a decreased AM participation in the lower PHN degradation pathway when being part of the consortium. The fact that HNA was efficiently metabolized by SC-1

is an important observation for considering this consortium as the most efficient for bioremediation purposes.

Two candidates able to initiate PHN attack (AM and Bk) were present in SC-4, probably suggesting competition with each other (Fig. 3). However, the metaproteomic analysis showed a significant protein expression of the AM strain in all the steps of the pathway in SC-4, demonstrating that AM participated in PHN degradation in both consortia. In addition, two dioxygenase enzymes of AM, classified as A and B by RHObase, and other enzymes responsible for HNA attack (Tables S9 and S10) were overexpressed in SC-4, indicating a differential regulation of cellular proteins in AM in the presence of Bk. Accordingly, physiological situations influencing the expression of catabolic genes when bacteria share ecological niches should be further explored.

The metabolic roles of consortia members during PHN exposure were further studied using a metaproteomics approach, resulting in the identification of several proteins. Comparison of PAH degradation pathway regulated proteins between species revealed potential functional redundancy between AM and Bk strains regarding the initial PAH attack and metabolism of intermediates (Fig. 6**a** and Tables S9 and S10). The coexistence of *Sphingomonas* and *Burkholderia* species was also reported by other authors [24,71]. Dioxygenases of the Bk strain, classified as class A in RHObase, were also significantly expressed in SC-4, showing that Bk was actively participating in the initial PHN attack (Tables S9 and S10). The expression of salicylate hydroxylase in Bk, classified as C by RHObase, could catalyse both the hydroxylation of salicylate (step 19) and the conversion of HNA into 1,2-dihydroxynaphthalene (step 14) [57,65]. The expression of dioxygenases like homogentisate 1,2 (step 15) and catechol 2,3 (step 23) indicates that Bk also participated at the bottom of the PHN degradation pathway (Fig. 6**b** and Tables S9 and S10). Besides, HNA accumulation in SC-4 suggests a competition effect of AM, B, Bc-h, T and Inq strains with Bk, causing a decrease in the synergistic effect observed in SC-1 (Fig. 4). This could be linked to the bacterial composition of both consortia, were ASVs associated with Inq were detected at frequencies lower than 3 % across the whole experiment, indicating a shift to a lower relative density, possibly due to the predicted dependence of degradation of by-products.

Concordantly, the presence of the Bk strain significantly altered the protein expression pattern in SC-1 and SC-4, probably caused by the interaction of Bk with the other strains composing SC-4 (Fig. 6**a**). It has been established that the phenomenon of antagonism and competition could have a negative impact on the degrading capacity of a pollutant (in our case HNA) [72]. The competition effect or negative interaction between Bk and the others strains observed in SC-4 could also be present in CON, which showed a similar pattern of HNA accumulation (Fig. 4**e**). The underlying reason for this may be that the antagonisms among members of a specific consortium would prevent them from accomplishing a higher synergistic degradation [73].

Both SC showed a pronounced stress response and over-expression of different membrane transport systems mediated by proteins of all the strains during PHN degradation (Fig. 6**a** and Tables S9 and S10). Proteins with antioxidant function help in combating oxidative and osmotic stress [74] and were previously observed during PAH metabolism [26] as a result of the production of oxidative damage by oxygenases involved in the degradation of these compounds [75]. Membrane transport proteins like TonB-dependent active transporter, play a crucial role in aromatic degradation in Gram-negative bacteria, allowing the transport of large molecules across the cell membrane [76,77].

5. Conclusion

The results obtained in our study clearly confirm the advantages of synthetic consortia over individual populations, and even over natural consortia, in the biodegradation of complex pollutants, highlighting the relevance of interactions and functional redundancy in natural environmental conditions. From a technological point of view, this is very important since synthetic bacterial assemblages can be propagated more easily than natural consortia under carefully maintained experimental conditions [78]. The selection of microorganisms for consortium design was essential to optimize its degradation efficiency. In particular, SC-1 turned out to be the most efficient for PAH degradation in liquid culture and it would be therefore interesting to test its performance as an inoculant in PAH-contaminated soils. Overall, the current results could help us improve the design and study of minimal functional bacterial consortia with the strains studied.

Funding information

Declaration of Competing Interest

The authors declare that they have no known competing financial interests or personal relationships that could have appeared to influence the work reported in this paper.

Appendix A. Supplementary data

Supplementary material related to this article can be found, in the online version, at doi:https://doi.org/10.1016/j.btre.2021.e00588.

References

[1] V. Smil, Examining energy transitions: a dozen insights based on performance, Energy Res. Soc. Sci. 22 (2016) 194–197, doi:http://dx.doi.org/10.1016/j.erss.2016.08.017.

[2] O.O. Alegbeleye, B.O. Opeolu, V.A. Jackson, Polycyclic aromatic hydrocarbons: a critical review of environmental occurrence and bioremediation, Environ. Manage. 60 (2017) 758–783, doi:http://dx.doi.org/10.1007/s00267-017-0896-2.

[3] D. Ghosal, S. Ghosh, T.K. Dutta, Y. Ahn, Current state of knowledge in microbial degradation of polycyclic aromatic hydrocarbons (PAHs): A review, Front. Microbiol. 7 (2016), doi:http://dx.doi.org/10.3389/fmicb.2016.01369.

[4] R.L. Shahab, J.S. Luterbacher, S. Brethauer, M.H. Studer, Consolidated bioprocessing of lignocellulosic biomass to lactic acid by a synthetic fungal-bacterial consortium, Biotechnol. Bioeng. 115 (2018) 1207–1215, doi:http://dx.doi.org/10.1002/bit.26541.

[5] P.E. Puentes-Téllez, J. Falcao Salles, Construction of effective minimal active microbial consortia for lignocellulose degradation, Microb. Ecol. 76 (2018) 419–429, doi:http://dx.doi.org/10.1007/s00248-017-1141-5.

[6] M. Cavaliere, S. Feng, O.S. Soyer, J.I. Jiménez, Cooperation in microbial communities and their biotechnological applications, Environ. Microbiol. 19 (2017) 2949–2963, doi:http://dx.doi.org/10.1111/1462-2920.13767.

[7] Q. Ma, Y.H. Bi, E.X. Wang, B.B. Zhai, X.T. Dong, B. Qiao, M.Z. Ding, Y.J. Yuan, Integrated proteomic and metabolomic analysis of a reconstructed three-species microbial consortium for one-step fermentation of 2-keto-l-gulonic acid, the precursor of vitamin C, J. Ind. Microbiol. Biotechnol. 46 (2019) 21–31, doi:http://dx.doi.org/10.1007/s10295-018-2096-3.

[8] N. Das, P. Chandran, Microbial degradation of petroleum hydrocarbon contaminants: an overview, Biotechnol. Res. Int. 2011 (2011) 1–13, doi:http://dx.doi.org/10.4061/2011/941810.

[9] G. Gupta, V. Kumar, A.K. Pal, Microbial degradation of high molecular weight polycyclic aromatic hydrocarbons with emphasis on pyrene, Polycycl. Aromat. 0 (2017) 1–13, doi:http://dx.doi.org/10.1080/10406638.2017.1293696.

[10] E.A. Del Rio-Chanona, X. Cong, E. Bradford, D. Zhang, K. Jing, Review of advanced physical and data-driven models for dynamic bioprocess simulation: case study of algae–bacteria consortium wastewater treatment, Biotechnol. Bioeng. 116 (2019) 342–353, doi:http://dx.doi.org/10.1002/bit.26881.

[11] S. Ben Said, D. Or, Synthetic microbial ecology: engineering habitats for modular consortia, Front. Microbiol. 8 (2017), doi:http://dx.doi.org/10.3389/fmicb.2017.01125.

[12] T. Großkopf, O.S. Soyer, Synthetic microbial communities, Curr. Opin. Microbiol. 18 (2014) 72–77, doi:http://dx.doi.org/10.1016/j.mib.2014.02.002.

[13] H. Song, M.-Z. Ding, X.-Q. Jia, Q. Ma, Y.-J. Yuan, Synthetic microbial consortia: from systematic analysis to construction and applications, Chem. Soc. Rev. 43 (2014) 6954–6981, doi:http://dx.doi.org/10.1039/C4CS00114A.

[14] S.R. Lindemann, H.C. Bernstein, H.S. Song, J.K. Fredrickson, M.W. Fields, W. Shou, D.R. Johnson, A.S. Beliaev, Engineering microbial consortia for controllable outputs, ISME J. 10 (2016) 2077–2084, doi:http://dx.doi.org/10.1038/ismej.2016.26.

[15] S.A. Shetty, H. Smidt, W.M. de Vos, Reconstructing functional networks in the human intestinal tract using synthetic microbiomes, Curr. Opin. Biotechnol. 58 (2019) 146–154, doi:http://dx.doi.org/10.1016/j.copbio.2019.03.009.

[16] J. Herschend, Z.B.V. Damholt, A.M. Marquard, B. Svensson, S.J. Sørensen, P. Hägglund, M. Burmølle, A meta-proteomics approach to study the interspecies interactions affecting microbial biofilm development in a model community, Sci. Rep. 7 (2017), doi:http://dx.doi.org/10.1038/s41598-017-16633-6.

[17] R. Bargiela, M. Ferrer, Metagenomics 1539 (2017) 145–157, doi:http://dx.doi.org/10.1007/978-1-4939-6691-2.

[18] H. Mikesková, C. Novotný, K. Svobodová, Interspecific interactions in mixed microbial cultures in a biodegradation perspective, Appl. Microbiol. Biotechnol. 95 (2012) 861–870, doi:http://dx.doi.org/10.1007/s00253-012-4234-6.

[19] M.A. Malla, A. Dubey, S. Yadav, A. Kumar, A. Hashem, E.F. Abd-Allah, Understanding and designing the strategies for the microbe-mediated remediation of environmental contaminants using omics approaches, Front. Microbiol. 9 (2018), doi:http://dx.doi.org/10.3389/fmicb.2018.01132.

[20] K.D. Brune, T.S. Bayer, Engineering microbial consortia to enhance biomining and bioremediation, Front. Microbiol. 3 (2012) 1–6, doi:http://dx.doi.org/10.3389/fmicb.2012.00203.

[21] J. Stadie, A. Gulitz, M.A. Ehrmann, R.F. Vogel, Metabolic activity and symbiotic interactions of lactic acid bacteria and yeasts isolated from water kefir, Food Microbiol. 35 (2013) 92–98, doi:http://dx.doi.org/10.1016/j.fm.2013.03.009.

[22] S. Festa, B.M. Coppotelli, I.S. Morelli, Bacterial diversity and functional interactions between bacterial strains from a phenanthrene-degrading consortium obtained from a chronically contaminated-soil, Int. Biodeterior. Biodegrad. 85 (2013) 42–51, doi:http://dx.doi.org/10.1016/j.ibiod.2013.06.006.

[23] S. Festa, M. Macchi, F. Cortés, I.S. Morelli, B.M. Coppotelli, Monitoring the impact of bioaugmentation with a PAH-degrading strain on different soil microbiomes using pyrosequencing, FEMS Microbiol. Ecol. 92 (2016) 1–12, doi:http://dx.doi.org/10.1093/femsec/fiw125.

[24] S. Festa, B.M. Coppotelli, L. Madueño, C.L. Loviso, M. Macchi, R.M. Neme Tauil, M.P. Valacco, I.S. Morelli, Assigning ecological roles to the populations belonging to a phenanthrene-degrading bacterial consortium using omic approaches, PLoS One 12 (2017) 1–21, doi:http://dx.doi.org/10.1371/journal.pone.0184505.

[25] P. Entcheva, Wolfgang Liebl, A. Johann, T. Hartsch, W.R. Streit, Direct cloning from enrichment cultures, a reliable strategy for isolation of complete operons and genes from microbial consortia, Appl. Environ. Microbiol. 67 (2001) 89–99, doi:http://dx.doi.org/10.1128/AEM.67.1.89-99.2001.

[26] M. Macchi, M. Martinez, R.M.N. Tauil, M.P. Valacco, I.S. Morelli, B.M. Coppotelli, Insights into the genome and proteome of Sphingomonas paucimobilis strain 20006FA involved in the regulation of polycyclic aromatic hydrocarbon degradation, World J. Microbiol. Biotechnol. 34 (2018) 0, doi:http://dx.doi.org/10.1007/s11274-017-2391-6.

[27] J. Chakraborty, T. Jana, S. Saha, T.K. Dutta, Ring-Hydroxylating oxygenase database: a database of bacterial aromatic ring-hydroxylating oxygenases in the management of bioremediation and biocatalysis of aromatic compounds, Environ. Microbiol. Rep. 6 (2014) 519–523, doi:http://dx.doi.org/10.1111/1758-2229.12182.

[28] M.A. Larkin, G. Blackshields, N.P. Brown, R. Chenna, P.A. Mcgettigan, H. McWilliam, F. Valentin, I.M. Wallace, A. Wilm, R. Lopez, J.D. Thompson, T.J. Gibson, D.G. Higgins, Clustal W and clustal X version 2.0, Bioinformatics 23 (2007) 2947–2948, doi:http://dx.doi.org/10.1093/bioinformatics/btm404.

[29] D.T. Jones, W.R. Taylor, J.M. Thornton, The rapid generation of mutation data matrices, Bioinformatics 8 (1992) 275–282, doi:http://dx.doi.org/10.1093/bioinformatics/8.3.275.

[30] S. Kumar, G. Stecher, M. Li, C. Knyaz, K. Tamura, MEGA X: molecular evolutionary genetics analysis across computing platforms, Mol. Biol. Evol. 35 (2018) 1547–1549, doi:http://dx.doi.org/10.1093/molbev/msy096.

[31] M. Duarte, R. Jauregui, R. Vilchez-Vargas, H. Junca, D.H. Pieper, AromaDeg, a novel database for phylogenomics of aerobic bacterial degradation of aromatics, Database 2014 (2014) 1–12, doi:http://dx.doi.org/10.1093/database/bau118.

[32] M. Kanehisa, S. Goto, Y. Sato, M. Kawashima, M. Furumichi, M. Tanabe, Data, information, knowledge and principle: back to metabolism in KEGG, Nucleic Acids Res. 42 (2014) 199–205, doi:http://dx.doi.org/10.1093/nar/gkt1076.

[33] A. Bateman, M.J. Martin, C. O'Donovan, M. Magrane, R. Apweiler, E. Alpi, R. Antunes, J. Arganiska, B. Bely, M. Bingley, C. Bonilla, R. Britto, B. Bursteinas, G.

Chavali, E. Cibrian-Uhalte, A. Da Silva, M. De Giorgi, T. Dogan, F. Fazzini, P. Gane, L.G. Castro, P. Garmiri, E. Hatton-Ellis, R. Hieta, R. Huntley, D. Legge, W. Liu, J. Luo, A. Macdougall, P. Mutowo, A. Nightingale, S. Orchard, K. Pichler, D. Poggioli, S. Pundir, L. Pureza, G. Qi, S. Rosanoff, R. Saidi, T. Sawford, A. Shypitsyna, E. Turner, V. Volynkin, T. Wardell, X. Watkins, H. Zellner, A. Cowley, L. Figueira, W. Li, H. McWilliam, R. Lopez, I. Xenarios, L. Bougueleret, A. Bridge, S. Poux, N. Redaschi, L. Aimo, G. Argoud-Puy, A. Auchincloss, K. Axelsen, P. Bansal, D. Baratin, M.C. Blatter, B. Boeckmann, J. Bolleman, E. Boutet, L. Breuza, C. Casal-Casas, E. De Castro, E. Coudert, B. Cuche, M. Doche, D. Dornevil, S. Duvaud, A. Estreicher, L. Famiglietti, M. Feuermann, E. Gasteiger, S. Gehant, V. Gerritsen, A. Gos, N. Gruaz-Gumowski, U. Hinz, C. Hulo, F. Jungo, G. Keller, V. Lara, P. Lemercier, D. Lieberherr, T. Lombardot, X. Martin, P. Masson, A. Morgat, T. Neto, N. Nouspikel, S. Paesano, I. Pedruzzi, S. Pilbout, M. Pozzato, M. Pruess, C. Rivoire, B. Roechert, M. Schneider, C. Sigrist, K. Sonesson, S. Staehli, A. Stutz, S. Sundaram, M. Tognolli, L. Verbregue, A.L. Veuthey, C.H. Wu, C.N. Arighi, L. Arminski, C. Chen, Y. Chen, J.S. Garavelli, H. Huang, K. Laiho, P. McGarvey, D.A. Natale, B.E. Suzek, C.R. Vinayaka, Q. Wang, Y. Wang, L.S. Yeh, M.S. Yerramalla, J. Zhang, UniProt: a hub for protein information, Nucleic Acids Res. 43 (2015) D204–D212, doi:http://dx.doi.org/10.1093/nar/gku989.

[34] C. Camacho, G. Coulouris, V. Avagyan, N. Ma, J. Papadopoulos, K. Bealer, T.L. Madden, BLAST+: architecture and applications, BMC Bioinformatics 10 (2009) 1–9, doi:http://dx.doi.org/10.1186/1471-2105-10-421.

[35] R.M. Waterhouse, F. Tegenfeldt, J. Li, E.M. Zdobnov, E.V. Kriventseva, OrthoDB: a hierarchical catalog of animal, fungal and bacterial orthologs, Nucleic Acids Res. 41 (2012) 358–365, doi:http://dx.doi.org/10.1093/nar/gks1116.

[36] S. Hunter, R. Apweiler, T.K. Attwood, A. Bairoch, A. Bateman, D. Binns, P. Bork, U. Das, L. Daugherty, L. Duquenne, R.D. Finn, J. Gough, D. Haft, N. Hulo, D. Kahn, E. Kelly, A. Laugraud, I. Letunic, D. Lonsdale, R. Lopez, M. Madera, J. Maslen, C. Mcanulla, J. McDowall, J. Mistry, A. Mitchell, N. Mulder, D. Natale, C. Orengo, A. F. Quinn, J.D. Selengut, C.J.A. Sigrist, M. Thimma, P.D. Thomas, F. Valentin, D. Wilson, C.H. Wu, C. Yeats, InterPro: the integrative protein signature database, Nucleic Acids Res. 37 (2009) 211–215, doi:http://dx.doi.org/10.1093/nar/gkn785.

[37] R.D. Finn, A. Bateman, J. Clements, P. Coggill, R.Y. Eberhardt, S.R. Eddy, A. Heger, K. Hetherington, L. Holm, J. Mistry, E.L.L. Sonnhammer, J. Tate, M. Punta, Pfam: the protein families database, Nucleic Acids Res. 42 (2014) 222–230, doi:http://dx.doi.org/10.1093/nar/gkt1223.

[38] P. Shannon, A. Markiel, Owen Ozier, N.S. Baliga, J.T. Wang, D. Ramage, N. Amin, B. Schwikowski, T. Ideker, Cytoscape: a software environment for integrated models of biomolecular interaction networks, Genome Res. (2003) 2498–2504, doi:http://dx.doi.org/10.1101/gr.1239303.metabolite.

[39] G.I. Vecchioli, M.T. Del Panno, M.T. Painceira, Use of selected autochthonous soil bacteria to enhanced degradation of hydrocarbons in soil, Environ. Pollut. 67 (1990) 249–258, doi:http://dx.doi.org/10.1016/0269-7491(90)90190-N.

[40] X.Q. Tao, G.N. Lu, Z. Dang, C. Yang, X.Y. Yi, A phenanthrene-degrading strain Sphingomonas sp. GY2B isolated from contaminated soils, Process Biochem. 42 (2007) 401–408, doi:http://dx.doi.org/10.1016/j.procbio.2006.09.018.

[41] B.M. Coppotelli, A. Ibarrolaza, R.L. Dias, M.T. Del Panno, L. Berthe-Corti, I.S. Morelli, Study of the degradation activity and the strategies to promote the bioavailability of phenanthrene by Sphingomonas paucimobilis Strain 20006FA, Microb. Ecol. 59 (2010) 266–276, doi:http://dx.doi.org/10.1007/s00248-009-9563-3.

[42] A. Camarinha-Silva, R. Jáuregui, D. Chaves-Moreno, A.P.A. Oxley, F. Schaumburg, K. Becker, M.L. Wos-Oxley, D.H. Pieper, Comparing the anterior nare bacterial community of two discrete human populations using Illumina amplicon sequencing, Environ. Microbiol. 16 (2014) 2939–2952, doi:http://dx.doi.org/10.1111/1462-2920.12362.

[43] D. Chaves-Moreno, I. Plumeier, S. Kahl, B. Krismer, A. Peschel, A.P.A. Oxley, R. Jauregui, D.H. Pieper, The microbial community structure of the cotton rat nose, Environ. Microbiol. Rep. 7 (2015) 929–935, doi:http://dx.doi.org/10.1111/1758-2229.12334.

[44] P. Khara, M. Roy, J. Chakraborty, D. Ghosal, T.K. Dutta, Functional characterization of diverse ring-hydroxylating oxygenases and induction of complex aromatic catabolic gene clusters in Sphingobium sp, PNB. FEBS Open Bio 4 (2014) 290–300, doi:http://dx.doi.org/10.1016/j.fob.2014.03.001.

[45] K.J. Livak, T.D. Schmittgen, Analysis of relative gene expression data using real-time quantitative PCR and the $2-\Delta\Delta CT$ method, Methods 25 (2001) 402–408, doi:http://dx.doi.org/10.1006/meth.2001.1262.

[46] Y. Perez-riverol, A. Csordas, J. Bai, M. Bernal-llinares, S. Hewapathirana, D.J. Kundu, A. Inuganti, J. Griss, G. Mayer, M. Eisenacher, P. Enrique, J. Uszkoreit, J. Pfeuffer, S. Tiwary, E. Audain, M. Walzer, A.F. Jarnuczak, T. Ternent, A. Brazma, A. Vizca, The PRIDE database and related tools and resources in 2019 : improving support for quantification data, Nucleic Acids Res. 47 (2019) 442–450, doi:http://dx.doi.org/10.1093/nar/gky1106.

[47] K. Shinoda, M. Tomita, Y. Ishihama, emPAI Calc-for the estimation of protein abundance from large-scale identification data by liquid chromatography-tandem mass spectrometry, Bioinformatics 26 (2009) 576–577, doi:http://dx.doi.org/10.1093/bioinformatics/btp700.

[48] S. Festa, B.M. Coppotelli, I.S. Morelli, Comparative bioaugmentation with a consortium and a single strain in a phenanthrene-contaminated soil: impact on the bacterial community and biodegradation, Agric., Ecosyst. Environ., Appl. Soil Ecol. 98 (2016) 8–19, doi:http://dx.doi.org/10.1016/j.apsoil.2015.08.025.

[49] W. Dejonghe, N. Boon, D. Seghers, E.M. Top, W. Verstraete, Bioaugmentation of soils by increasing microbial richness: missing links, Environ. Microbiol. 3 (2001) 649–657, doi:http://dx.doi.org/10.1046/j.1462-2920.2001.00236.x.

[50] X. Jia, C. Liu, H. Song, M. Ding, J. Du, Q. Ma, Y. Yuan, Design, analysis and application of synthetic microbial consortia, Synth. Syst. Biotechnol. 1 (2016) 109–117, doi:http://dx.doi.org/10.1016/j.synbio.2016.02.001.

[51] Y. Ohtsubo, A. Moriya, H. Kato, N. Ogawa, Y. Nagata, M. Tsuda, Complete genome sequence of a phenanthrene degrader, Genome Announc. 3 (2015) 2014–2015, doi:http://dx.doi.org/10.1128/genomeA.01283-15.Copyright.

[52] O. Ponomarova, K.R. Patil, Metabolic interactions in microbial communities: untangling the Gordian knot, Curr. Opin. Microbiol. 27 (2015) 37–44, doi:http://dx.doi.org/10.1016/j.mib.2015.06.014.

[53] R. Vilchez-Vargas, H. Junca, D.H. Pieper, Metabolic networks, microbial ecology and "omics" technologies: towards understanding in situ biodegradation processes, Environ. Microbiol. 12 (2010) 3089–3104, doi:http://dx.doi.org/10.1111/j.1462-2920.2010.02340.x.

[54] A. Cébron, M.P. Norini, T. Beguiristain, C. Leyval, Real-Time PCR quantification of PAH-ring hydroxylating dioxygenase (PAH-RHDα) genes from Gram positive and Gram negative bacteria in soil and sediment samples, J. Microbiol. Methods 73 (2008) 148–159, doi:http://dx.doi.org/10.1016/j.mimet.2008.01.009.

[55] M.S. Marcos, M. Lozada, H.M. Dionisi, Aromatic hydrocarbon degradation genes from chronically polluted Subantarctic marine sediments, Lett. Appl. Microbiol. 49 (2009) 602–608, doi:http://dx.doi.org/10.1111/j.1472-765X.2009.02711.x.

[56] T.P. Sipilä, A.K. Keskinen, M.L. Åkerman, C. Fortelius, K. Haahtela, K. Yrjälä, High aromatic ring-cleavage diversity in birch rhizosphere: PAH treatment-specific changes of I.E.3 group extradiol dioxygenases and 16S rRNA bacterial communities in soil, ISME J. 2 (2008) 968–981, doi:http://dx.doi.org/10.1038/ismej.2008.50.

[57] O. Cho, K.Y. Choi, G.J. Zylstra, Y.S. Kim, S.K. Kim, J.H. Lee, H.Y. Sohn, G.S. Kwon, Y. M. Kim, E. Kim, Catabolic role of a three-component salicylate oxygenase from Sphingomonas yanoikuyae B1 in polycyclic aromatic hydrocarbon degradation, Biochem. Biophys. Res. Commun. 327 (2005) 656–662, doi:http://dx.doi.org/10.1016/j.bbrc.2004.12.060.

[58] T.M. Neher, D.R. Lueking, Pseudomonas fluorescens ompW : plasmid localization and requirement for naphthalene uptake, Can. J. Microbiol. 55 (2009) 553–563, doi:http://dx.doi.org/10.1139/w09-002.

[59] C. Kazunga, M.D. Aitken, Products from the incomplete metabolism of pyrene by polycyclic aromatic hydrocarbon-degrading bacteria, Appl. Environ. Microbiol. 66 (2000) 1917–1922, doi:http://dx.doi.org/10.1128/AEM.66.5.1917-1922.2000.

[60] J.S. Seo, Y.S. Keum, Y. Hu, S.E. Lee, Q.X. Li, Degradation of phenanthrene by Burkholderia sp. C3: initial 1,2- and 3,4-dioxygenation and meta- and ortho-cleavage of naphthalene-1,2-diol, Biodegradation 18 (2007) 123–131, doi:http://dx.doi.org/10.1007/s10532-006-9048-8.

[61] J. Deveryshetty, P.S. Phale, Biodegradation of phenanthrene by Alcaligenes sp. strain PPH: Partial purification and characterization of 1-hydroxy-2-naphthoic acid hydroxylase, FEMS Microbiol. Lett. 311 (2010) 93–101, doi:http://dx.doi.org/10.1111/j.1574-6968.2010.02079.x.

[62] Y. Jouanneau, J. Micoud, C. Meyer, Purification and characterization of a three-component salicylate 1-hydroxylase from Sphingomonas sp. strain CHY-1, Appl. Environ. Microbiol. 73 (2007) 7515–7521, doi:http://dx.doi.org/10.1128/AEM.01519-07.

[63] M. Duarte, A. Nielsen, A. Camarinha-Silva, R. Vilchez-Vargas, T. Bruls, M.L. Wos-Oxley, R. Jauregui, D.H. Pieper, Functional soil metagenomics: elucidation of polycyclic aromatic hydrocarbon degradation potential following 12 years of in situ bioremediation, Environ. Microbiol. 19 (2017) 2992–3011, doi:http://dx.doi.org/10.1111/1462-2920.13756.

[64] I.F. Puntus, A.E. Filonov, L.I. Akhmetov, A.V. Karpov, A.M. Boronin, Phenanthrene degradation by bacteria of the genera Pseudomonas and Burkholderia in model soil systems, Microbiology 77 (2008) 7–15, doi:http://dx.doi.org/10.1007/s11021-008-1002-9.

[65] N.V. Balashova, A. Stolz, H.J. Knackmuss, I.A. Kosheleva, A.V. Naumov, A.M. Boronin, Purification and characterization of a salicylate hydroxylase involved in 1-hydroxy-2-naphthoic acid hydroxylation from the naphthalene and phenanthrene-degrading bacterial strain Pseudomonas putida BS202-P1, Biodegradation 12 (2001) 179–188, doi:http://dx.doi.org/10.1023/A:1013126723719.

[66] M. Lin, X. Hu, W. Chen, H. Wang, C. Wang, Biodegradation of phenanthrene by Pseudomonas sp: BZ-3, isolated from crude oil contaminated soil, Int. Biodeterior. Biodegrad. 94 (2014) 176–181, doi:http://dx.doi.org/10.1016/j.ibiod.2014.07.011.

[67] J.H. Lawton, V.K. Brown, Redundancy in ecosystems, Biodivers. Ecosyst. Funct. (1994) 255–270, doi:http://dx.doi.org/10.1007/978-3-642-58001-7_12.

[68] J.S. Rosenfeld, Functional redundancy in ecology and conservation, Oikos 98 (2002) 156–162, doi:http://dx.doi.org/10.1034/j.1600-0706.2002.980116.x.

[69] S. Vaidya, K. Jain, D. Madamwar, Metabolism of pyrene through phthalic acid pathway by enriched bacterial consortium composed of Pseudomonas, Burkholderia, and Rhodococcus (PBR), 3 Biotech 7 (2017), doi:http://dx.doi.org/10.1007/s13205-017-0598-8.

[70] P. Wanapaisan, N. Laothamteep, F. Vejarano, J. Chakraborty, M. Shintani, C. Muangchinda, T. Morita, C. Suzuki-Minakuchi, K. Inoue, H. Nojiri, O. Pinyakong, Synergistic degradation of pyrene by five culturable bacteria in a mangrove sediment-derived bacterial consortium, J. Hazard. Mater. 342 (2018) 561–570, doi:http://dx.doi.org/10.1016/j.jhazmat.2017.08.062.

[71] G.G. Willsey, M.J. Wargo, Extracellular lipase and protease production from a model drinking water bacterial community is functionally robust to absence of

individual members, PLoS One 10 (2015) 1–15, doi:http://dx.doi.org/10.1371/journal.pone.0143617.

[72] M.S. Fuentes, G.E. Briceño, J.M. Saez, C.S. Benimeli, M.C. Diez, M.J. Amoroso, Enhanced removal of a pesticides mixture by single cultures and consortia of free and immobilized streptomyces strains, Biomed Res. Int. 2013 (2013), doi: http://dx.doi.org/10.1155/2013/392573.

[73] K. Patowary, R. Patowary, M.C. Kalita, S. Deka, Development of an efficient bacterial consortium for the potential remediation of hydrocarbons from contaminated sites, Front. Microbiol. 7 (2016) 1–14, doi:http://dx.doi.org/10.3389/fmicb.2016.01092.

[74] L. Masip, K. Veeravalli, G. Georgiou, The many faces of glutathione in Bacteria, Geogr. J. 176 (2010) 267–269, doi:http://dx.doi.org/10.1111/j.1475-4959.2010.00371.x.

[75] B. Favaloro, A. Tamburro, M.A. Trofino, L. Bologna, D. Rotilio, H.J. Heipieper, Modulation of the glutathione S-transferase in Ochrobactrum anthropi:

[76] F. Hua, H.Q. Wang, Uptake and trans-membrane transport of petroleum hydrocarbons by microorganisms, Biotechnol. Biotechnol. Equip. 28 (2014) 165–175, doi:http://dx.doi.org/10.1080/13102818.2014.906136.

function of xenobiotic substrates and other forms of stress, Biochem. J. 346 (2000) 553–559, doi:http://dx.doi.org/10.1042/0264-6021:3460553.

[77] C. Perruchon, S. Vasileiadis, C. Rousidou, E. Papadopoulou, G. Tanou, M. Samiotaki, C. Garagounis, A. Molassiotis, K. Papadopoulou, D.G. Karpouzas, Metabolic pathway and cell adaptation mechanisms revealed through genomic, proteomic and transcription analysis of a Sphingomonas haloaromaticamans strain degrading ortho-phenylphenol, Sci. Rep. 7 (2017) 1–14, doi:http://dx.doi.org/10.1038/s41598-017-06727-6.

[78] J. Dolinšek, F. Goldschmidt, D.R. Johnson, Synthetic microbial ecology and the dynamic interplay between microbial genotypes, FEMS Microbiol. Rev. 40 (2016) 961–979, doi:http://dx.doi.org/10.1093/femsre/fuw024.